Electrochemical capacity of Ni mass when subjected to various conditions, and the relation to changes in the nickel hydroxide phase and crystallite size

- a Master's thesis at SAFT in Oskarshamn

By
Magnus Hedlund

Centre for Analysis and Synthesis, Department of Chemistry
Lund University

March 2016

Supervisor: **Rune Sjövall, SAFT AB**
Assistant Supervisor: **Professor Staffan Hansen**
Examiner: **Professor Sven Lidin**

Preface

I am very grateful to have gotten the opportunity to doing my thesis work at SAFT AB in Oskarshamn, and to get an insight of how work is done in an industry.
With this said I want to thank everyone in the production- and chemistry laboratories at SAFT for helping me understand how things work and for being patient with my questions and interruptions in their daily work.

A special thanks to my supervisor Rune for the support and the interesting and helpful discussions we had during the evenings.

I want to thank Professor Staffan Hansen for being my supervisor at the university even though I disappeared almost immediately to work on this in Oskarshamn.

Thank you, Professor Sven Lidin for accepting the role as my examiner, the helpful advice and interesting questions.

Abstract

The electrochemical capacity of the nickel mass in the positive electrode when subjected to various conditions, and the relation to changes in the nickel hydroxide phases and crystallite size was studied in this thesis work.
The various conditions being: two different electrolytes, KOH and KOH/LiOH, different temperature during charging and different charge times.
The nickel mass was made into monopockets to subject it to these conditions and register the capacity of the mass in a computer, which was connected to the charging station.
From the monopocket analysis it could be seen that for most samples the capacity increased with increasing charge time.
When the monopocket tests were done, the testing electrodes were cut open to analyse them in an X-ray diffractometer (XRD) to see what nickel hydroxide phases were present in the samples.
The analyses showed that the electrolyte with LiOH added to it was more prone to form γ-phase and generated smaller crystallite sizes than the electrolyte without this addition.
When comparing the monopocket results and the results from the XRD, it could be seen that the samples with KOH as electrolyte that had lower capacity than expected also had larger amounts of γ-phase. This implies that there was some loss of contact in the active material due to the swelling connected with the γ-phase.
When cycling the monopockets further than the standard three times, it was found that the samples that used pure KOH as electrolyte still had γ-phase residues left even after the twentieth cycle whilst the samples with LiOH added to the electrolyte had no γ-phase left.
The temperature testing gave a bit inconclusive results but the electrolyte with LiOH additions was clearly superior during these tests, which was no surprise as it has been found to improve the performance of the positive electrode at higher temperatures [3].

Sammanfattning

Den elektrokemiska kapaciteten för nickelmassan i den positiva elektroden när den blev utsatt för olika förhållande och dess relation till ändringar i nickelhydroxidfaser och kristallitstorlek undersöktes i detta examensarbete.
De olika förhållandena var: två olika elektrolyter, KOH och KOH/LiOH, olika temperaturer under laddning och olika laddningstider.
Nickelmassan gjordes till enfickor för att utsätta den för de olika förhållandena och dess kapacitet blev registrerad på en dator, som var kopplad till laddningsstationen.
Från enficksanalysen kunde man se att de flesta provernas kapacitet ökade med ökad laddningstid.
När enfickstesterna var klara, klipptes testelektroderna upp för att kunna analysera dem i en röntgendiffraktometer för att se vilka nickelhydroxidfaser som fanns i proverna.
Analysen visade att elektrolyten med LiOH tillsatt var mer benägen att bilda γ-fas och genererade mindre kristallitstorlekar än vad elektrolyten utan denna tillsats gjorde.
Vid jämförelse mellan enficksresultaten och resultaten från röntgendiffraktometern visade det sig att proverna med elektrolyten KOH som hade lägre kapacitet än förväntat också hade större mängder av γ-fas. Detta indikerar att det var en viss förlust av kontakt i det aktiva matrialet på grund av uppsvällningen kopplad till γ-fasen.
När enfickorna kördes tjugo cykler istället för de tre cykler som var standard, upptäcktes det att proverna som använde ren KOH som elektrolyt hade rester av γ-fas kvar även efter den tjugonde cykeln medan proverna med LiOH tillsatt till elektrolyten inte hade någon γ-fas kvar.
Temperaturförsöket gav ganska otydliga eller inkonsekventa resultat, men elektrolyten med LiOH tillsatsen var klart överlägsen under dessa försök, vilket inte var så konstigt då tidigare studier hade konstaterat att denna tillsats ökade prestandan av den positiva elektroden vid höga temperaturer [3].

Table of Contents

Introduction

In the current debate on minimizing the emissions and finding environmentally friendly sources of energy, what could be more relevant and interesting than batteries. Ni-Cd batteries have been around for a long time, supplying a reliable and stable answer to energy storage. They can function in very harsh environment due to the low freezing point of the electrolyte, allowing them to operate in temperatures between -40°C up to 60°C. This together with the ability to parallel circuit them makes them optimal, as back up power units for hospitals, airports or even smaller cities if power outage should strike.

The electrochemically active materials in Ni-Cd batteries are nickel- and cadmium mass, both being produced separately and independently at SAFT in Oskarshamn.

This thesis will focus on the nickel mass, which makes up the active material of the positive electrode.

Nickel hydroxide has been the subject for a lot of research; from understanding how the crystallite size is affecting the electrochemical properties [1] to investigate how different additives may change its properties or hinder different phases to occur [2]. This makes this thesis a compliment to the available research, as its aim is to study the electrochemical capacity of Ni mass in the positive electrode when subjected to various conditions and relate it to the nickel hydroxide phases and crystallite size. These conditions were two different electrolytes, KOH and KOH/LiOH, different temperature during the first charge (20°C → 40°C) and different charge times.

Theoretical Background

The electrochemical cell

The electrochemical cell contains three key components: positive electrode (cathode), electrolyte and negative electrode (anode), see figure 1. In this case the cathode is made out of $Ni(OH)_2$ and the anode is made out of $Cd(OH)_2$.

A battery consists of one or more electrochemical cells, each cell converting stored chemical energy to electrical energy. This conversion occurs in the form of spontaneous reduction-oxidation (redox) reactions transferring charged particles from the anode to the cathode during discharge, when the battery is connected to the load. Depending on the use of the battery the cell can be coupled together with other cells either in series or in parallel.

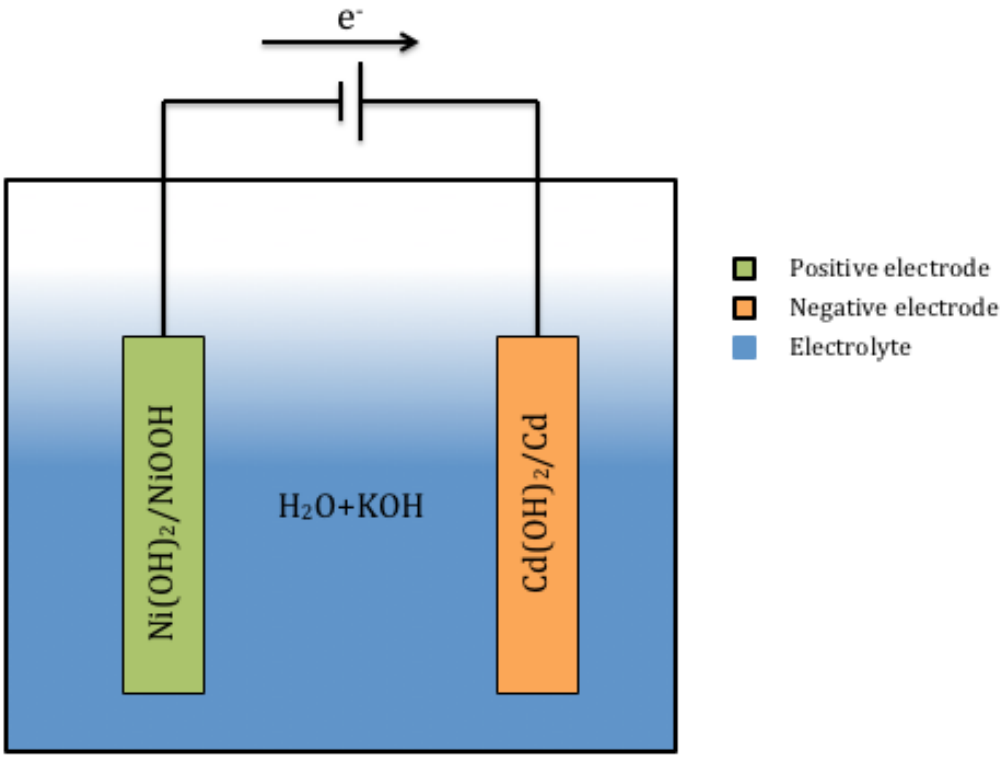

Figure 1. A schematic drawing of an electrochemical cell during charging. Inspired by an image in Christian's thesis [5].

Batteries can be divided into two categories, primary and secondary. The former being batteries that when the redox reaction reached its end, and all the active material in the electrodes has either been oxidised or reduced, are considered empty and are disposed of for recycling. The latter are batteries that, when they are empty, can be connected to an electrical source which reverses the redox reaction and restore them to their former state. The process of charging and discharging is called a cycle. During a cycle there is a risk that the battery looses some of its capacity, this can be due to formation of unwanted compounds or loss of contact with the active material.

Electrochemistry

During discharge the positive electrode (cathode) is reduced, meaning it receives electrons from the opposing, negative electrode (anode). By doing so the anode is oxidised and provides fuel for the electrochemical reaction. The purpose of the electrolyte is to assist the transfer of charged particles from the cathode to the anode but still remain, in principle, unaffected by the electrochemical processes that are occurring at the electrodes.

Active materials

Nickel, Ni

The positive electrode in discharged state is composed of nickel in the form of nickel hydroxide, which has been doped and modified to meet the battery requirements, and graphite as the conductive medium.
The nickel cycles between two oxidation states during charge and discharge, upon charge the nickel hydroxide is converted into nickel oxyhydroxide (NiOOH) through a deprotonation mechanism,

$$Ni(OH)_2 + OH^- \rightarrow NiOOH + H_2O + e^-$$

This reaction is reversed during discharge, reducing the 3+ nickel oxyhydroxide to 2+ nickel hydroxide, through protonation.

These two structures are called β-NiOOH and β-$Ni(OH)_2$ respectively, beta nickel hydroxide can ideally be described as a packing of nickel hydroxide in layers. The layers are built with edge sharing NiO_6 octahedra, where hydrogen atoms are located in the interlayer space in tetrahedral environments, above or below the oxygen atoms.

The beta nickel hydroxide is hexagonally close packed, with cell parameter *a* at 3,1 Å and parameter *c*, the interlayer distance, at 4,6 Å.
During charging one proton and one electron is removed from beta nickel hydroxide forming beta nickel oxyhydroxide, which has the same layered structure. The deprotonation results in a lowering of the cell parameter *a*, corresponding to the Ni-Ni distance, to 2,8 Å, due to the reduced ionic radius of Ni^{3+}, and parameter *c* is slightly increased to 4,7 Å as a result of a higher electrostatic repulsion between the nickel dioxide layers [3].

If it had been so simple that nickel hydroxide only took the shape of these two phases it would have been easy as they are the desired ones for battery usage, but nature is a cruel mistress and nickel hydroxide can form two additional phases depending on how its been handled during charge.
By overcharging β-NiOOH it becomes overoxidised leading to the formation of γ-NiOOH, which can reach an oxidation state of 3,6+.
As γ-phase forms the interlayer distance increases as a result of species (water molecules and solvated anions and cations) being intercalated. This swelling can reach an increase of nearly 50% of the interlayer distance, 4,6 Å to 7 Å. Electrolyte concentration and temperature affects the formation of this phase [3].

During discharge, the γ-phase is reduced to α-phase, this phase is unstable in concentrated alkaline solution resulting in the standard β-$Ni(OH)_2$ through a dissolution-precipitation mechanism, see figure 2.

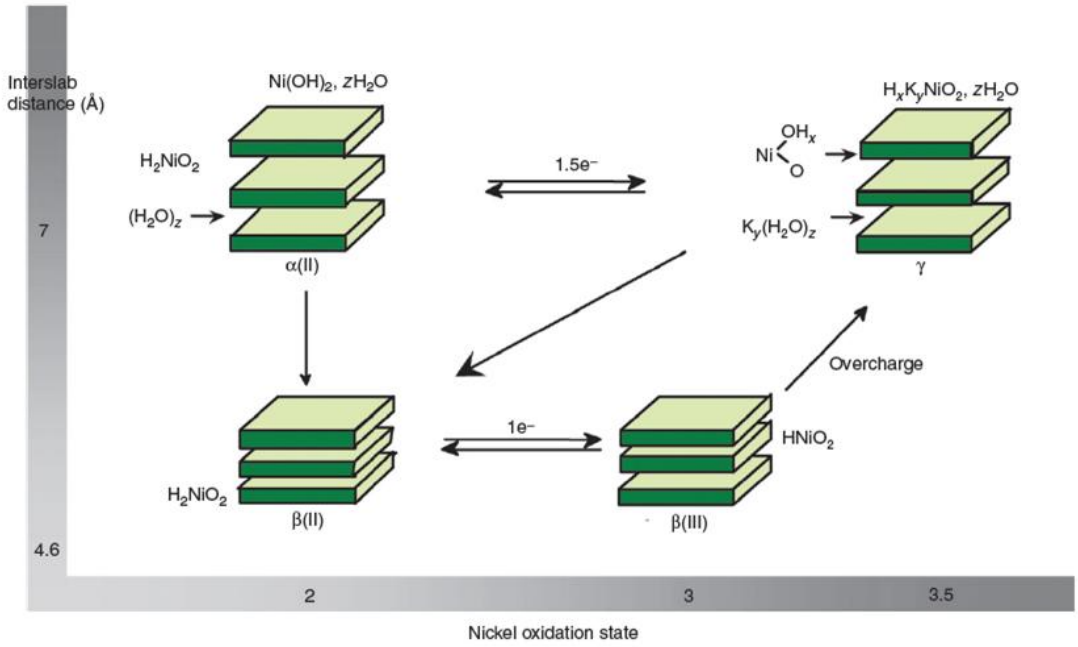

Figure 2. Structure and electrochemical reaction of nickel hydroxide and oxyhydroxide phases. Courtesy of Patrick Bernard [3].

In the alkaline environment of the electrolyte the positive nickel electrode has an equilibrium potential higher than the oxidation potential of water, which means it is above the stable window of the electrolyte. Thus the charged electrode is thermodynamically unstable and its stability is linked to the oxygen evolution overvoltage on the active material [3].

The theoretical maximum capacity of $Ni(OH)_2$ is 289 mAh/g, for the calculations see appendix A.

When adding LiOH to the electrolyte it can have beneficial effects on the performance of the battery, see Electrolyte section below, but it can also poison the positive nickel electrode by forming $LiNiO_2$. This is dependent on the amount of lithium in the electrolyte relative to the amount of nickel [8].

Cadmium, Cd

This thesis focuses on the positive electrode so it will only briefly describe the anode material and what reaction is taking place there, to give a theoretical background to how the batteries work.

The negative electrode consists of cadmium hydroxide, $Cd(OH)_2$, which during charging is reduced to metallic cadmium. The reaction is reversed throughout the discharge process, changing the oxidation state of cadmium from 0 to 2+, releasing two electrons per cadmium atom partaking in the reaction.
Below is the reaction for the anode during charge [3]

$$Cd(OH)_2 + 2e^- \rightarrow Cd + 2OH^-$$

Cadmium is a fairly hazardous metal by its own, therefore a series of regulations and guidelines on how to handle it are in place by both governments all over the world and the EU. The batteries produced and sold by SAFT are recycled for economic,

environmental and regulatory reasons. To ensure proper recycling, SAFT in Oskarshamn has its own recycling plant [4].

Competing reactions

As the charged positive nickel electrode is thermodynamically unstable in an alkaline environment, its stability is therefore linked to the oxygen evolution overvoltage on the active material. To charge the positive electrode to full capacity some overcharging is needed. This leads to competing reactions at the electrodes when the end of charge is reached, as mentioned below, and water electrolysis occurs [3].
On the negative electrode side, hydrogen evolution occurs according to this reaction,

$$4H_2O + 4e^- \rightarrow 2H_2{}^{\uparrow} + 4OH^-$$

And on the positive electrode side, oxygen evolution occurs according to this reaction,

$$4OH^- \rightarrow O_2{}^{\uparrow} + 2H_2O + 4e^-$$

The overall reaction can be written as,

$$2H_2O \rightarrow 2H_2{}^{\uparrow} + O_2{}^{\uparrow}$$

The overall reaction shows that during charging water is consumed and needs to be refilled so the battery can maintain its electrolyte concentration and electrochemical properties [3].

Electrolyte

The electrolyte acts as the ion charge carrier in batteries and for Ni-Cd batteries this mainly consists of concentrated potassium hydroxide, KOH, but may also have additions of sodium hydroxide, NaOH, and lithium hydroxide, LiOH.
The electrolyte concentration has an affect on the efficiency of the electrodes and the lifetime of the cell. High electrolyte concentration favours the α/γ-phases of the nickel electrode, which increases the efficiency of the positive electrode but also leads a swelling of the electrode and reduced lifetime of the cell [3]. The addition of sodium- and lithium hydroxide improves high-temperature performance of the positive electrode by increasing the interactions between electrolyte cations and water molecules due to the introduction of smaller cations. This leads to an increase in the electrolyte oxidation potential as the oxidation of the electrolyte becomes more difficult for Li^+ and Na^+ versus K^+ and thus increasing the oxygen evolution overvoltage [3].
Even though the electrolyte has an affect on the performance of the battery it is not part of the electrochemical reactions like in a lead-acid battery. Instead its sole purpose is to provide a way for the charged particles to travel from one electrode to the other.

Formation

The active materials for the electrodes are produced in the discharged state, meaning they are inactive. To activate the battery for the first time it goes through a process called formation, during formation the materials are charged with a very low charge rate, around C/5, to shape the internal components. This means a charge rate that will take five hours to reach the end voltage during discharge [9], [5].

Utilization

The utilization is a ratio, which measures the efficiency of the discharge process. A high utilization ratio or degree means that the charged energy of the battery can be accessed and drained easily. This would ensure a consistent output voltage throughout the discharge process, until the battery is drained. However, it might be difficult to access all the chemical energy at the target voltage. This residual energy is retrieved, but at a greatly reduced voltage [4], [5].

Note that the utilizations presented in this thesis are never stated in relation to the maximum theoretical capacity, but to the actual discharged capacity. The capacities used to calculate the utilization ratio are acquired at the relative voltage between the monopocket and the zinc rod equal to 1,5 V and 0,7 V.

X-ray diffraction

An X-ray diffractometer utilizes the diffraction effects that occur when X-rays interact with matter. The main components of an X-ray diffractometer are a source of X-rays, a monochromator, a sample holder and a detector.
The X-ray source emits photons, which travels through the monochromator to single out or narrow down the wavelength, λ, at an angle of θ relative to the sample (2θ relative to the detector). When the photons hit the sample, they are reflected on the planes of different unit cells. Since the photons have travelled different distances, they are no longer in phase. However, if the photons interact with the same unit cell, the difference in distance will be equal to an integer times the wavelength, the photons will be in phase and Bragg's law, equation below, will be satisfied resulting in constructive interference.

$$\lambda = 2d_{hkl} \sin \theta_{hkl}$$

This constructive interference leads to an increase in reflected photons registered by the detector, which results in a peak in the produced diffractogram. This peak can be used to determine the interplanar distance, d_{hkl}, for that interaction. As the angle of θ increases, more reflections may be registered, resulting in a number of peaks in the obtained diffractogram [6].

The peaks of importance for this thesis occurred at the angle of 2θ equal to 19,3° for plane 001 and 33,1° for plane 100 of $Ni(OH)_2$, 18,4° for plane 001 of β-NiOOH and 12,8° for plane 001 of γ-NiOOH. The big peak at 26,6° was from the graphite in the powder. For the samples with LiOH added to the electrolyte it could be interesting to look for the $LiNiO_2$, which would appear at the angle of 2θ equal to 18,8° for plane 001 [7].

The X-ray diffractometer at SAFT in Oskarshamn used Bragg-Brentano geometry, which means the X-ray source was fixed and the sample holder and detector rotated θ and 2θ, respectively.

Crystallite size

From these peaks in the diffractogram, the crystallite size could be calculated by utilizing the Scherrer equation, which can be seen below,

$$\tau = \frac{K\lambda}{\beta \cos\theta}$$

where:
τ is the mean size of crystallite
K is a dimensionless shape factor, typically with a value close to unity, 0.9 was used in this thesis, but varies with the actual shape of the crystallite.
λ is the X-ray wavelength
β is the line broadening at half maximum intensity (FWHM), after subtracting the instrumental line broadening, in radians.
θ is the Bragg angle

The instrumental line broadening had been established by XRD analysis of a quartz standard and subtracted from β.

The crystallite size of $Ni(OH)_2$ is related to the capacity of the electrode, if the yielded capacity is high the crystallite size becomes small and if the capacity is low the crystallite size becomes larger. This corresponds best to the 101 crystallites, but in this thesis the 001 crystallite size was studied [10].

Experimental Methods

Starting material

All materials used in this thesis were taken from the production facilities.
$Ni(OH)_2$ powder with a known capacity and crystallite size, was used as active material.
Two electrolytes, KOH and KOH/LiOH, with known concentrations, were used to examine how it would affect the capacity, crystallite size and nickel hydroxide phases.

Monopocket

Assembly

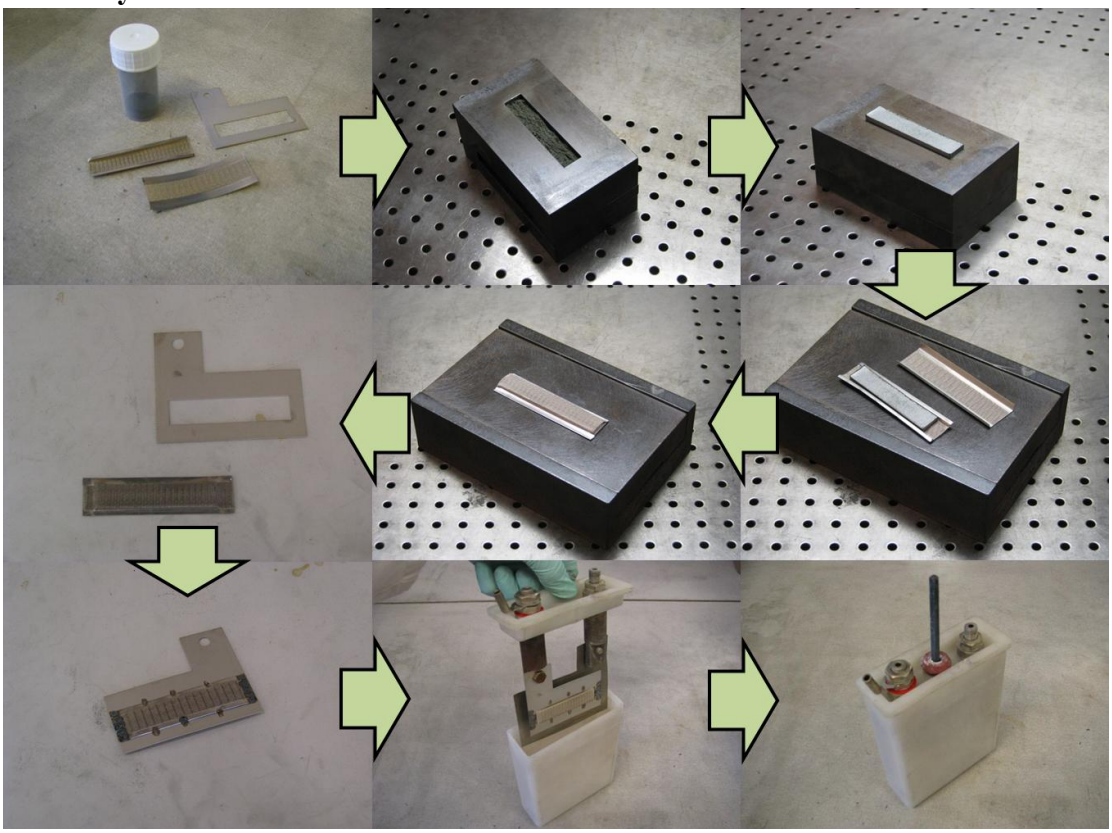

Figure 3. Images showing the process of assembling a monopocket, from powder to usable testing electrode. Courtesy of Christan Sundvall [5].

The process of assembling a monopocket can be seen in figure 3. Starting off with the active material in powder form mix together with graphite, as a conductive binder, all samples was weighed up to a uniform weight. The powder was then pressed into a briquette using a mould and a press machine, the pressure being the same for all samples. After that the briquette was placed on a perforated band of adequate length and covered by a similar band, which was clamped together to hold it in place. The result of these steps is a finish monopocket, but in this form it cannot be used as a testing electrode. Next the monopocket was point welded to a nickel plate and pressed in a mould with the pattern similar to that they use on the real electrodes in production. When this was done the plate was fastened to a grid and put in a plastic canister. The following section will cover the analysis.

Analysis

On the grid where the nickel plate with the monopocket was connected were also a nickel sheet connected. This sheet was used as a counter electrode, the anode, to the monopocket. However as it is an ordinary nickel sheet, it has no chemical energy stored and would therefore not make this assembly a functional battery.
Now that the monopocket could serve as an electrode, the canister was filled with electrolyte and a zinc rod in a plastic cylinder was placed between the monopocket and the sheet to avoid short circuit and the zinc rod was used as a reference electrode. When this was done the electrodes was connected to a charging station, which could be accessed via a computer. On the computer the monopocket could be evaluated using customizable programs simulating the charging/discharging process to see how

the material would behave under different conditions. During this evaluation, an electric current was introduced to or drained from the monopocket device. This current gives rise to potential differences within the cell, which is actually the purpose of this test; to measure the relative voltage between the monopocket, positive electrode, and the zinc rod. While there is no current flowing through the zinc rod, the relative voltage between the monopocket and the zinc rod can be used to estimate what voltage would be obtained had the active material of the monopocket been used in an actual battery [4], [5].

A typical program went through three cycles on the monopocket device, meaning charging and discharging three times. The charging times for the three cycles of the standard program were 12,5 h for the first, 9 h for the second and 7,5 h for the third cycle. The second cycles charge time was higher than the third to compensate for the deep discharge in the first cycle, which was done to acquire the capacity at 0,7 V so the utilization could be calculated for the first cycle.
To find the capacity of the active material, a data point where the voltage difference between the monopocket and the zinc rod equal to 1,5 V was used. This data point translates to roughly 1 V if the monopocket had been implemented in a proper Ni-Cd cell. The time it takes to pass this 1,5 V data point determines the capacity, in ampere-hours, Ah, of the active material. Furthermore, a data point at 0,7 V was also studied, as the ratio of these two points capacity gave the utilization, described earlier.

It was in this stage the monopockets were exposed to the different conditions that were studied in this thesis work.
The variation of the charge time was only set to the first charging and the charging in the second and third cycle remained the same for all samples.
To understand what phases were present in the active material after charging some of the test had the program stopped when the charge time of the first cycle was reached.
For the temperature testing the canisters were put in water baths of different temperature to reach 30 or 40°C. The canisters remained in the baths only during the first charging and when it was done they were picked up and cooled down to room temperature (20°C) before continuing with discharge and the following two cycles.
To analyse the effect of the electrolyte on the active material, the different electrolytes were added to the canisters before connecting them to the charging station and then letting the monopocket devices go through the programs.
The cycling tests were done as the room temperature tests but with modified programs so it would run for twenty cycles instead of the standard three, and some water was added to the canisters when the electrolyte levels was lower than the initial level.

Powder X-ray diffraction

The powder X-ray diffractometer used in this thesis work was a Panalytical (former Philips Analytical) X'pert with a Cu-Kα radiation source, it utilised the Bragg-Brentano geometry mentioned above. To analyse the surface of the samples the insides of the perforated bands were scraped and ground to a fine powder with a mortar and pestle. For the bulk samples the whole briquettes were ground in a mortar to a fine powder before put in the sample holder.

Results

Due to less importance to the thesis work, the diffractograms for the bulk samples can be found in appendix B.

The uncharged mass in the diffractograms refer to the pristine $Ni(OH)_2$ powder before it was made in to briquettes and electrochemically activated.

Table 1. Experimental plan showing the experiments presented in the results, X meaning that the experiment has been performed. The abbreviations refer to the sort of the experiment and where in results they can be found 1st Ch = first cycle charging, 3rd Dch = third cycle discharging and Cyc = cycling.

		Temperatures						
		20°C			30°C		40°C	
Electrolyte	Charge times	1st Ch	3rd Dch	Cyc	1st Ch	3rd Dch	1st Ch	3rd Dch
KOH	8 h	X	X	-	X	X	X	X
	10 h	X	X	X	X	X	X	X
	12,5 h	X	X	X	X	X	X	X
	24 h	X	X	X	X	X	X	X
KOH/LiOH	8 h	X	X	-	X	X	X	X
	10 h	X	X	X	X	X	X	X
	12,5 h	X	X	X	X	X	X	X
	24 h	X	X	X	X	X	X	X

First cycle charging

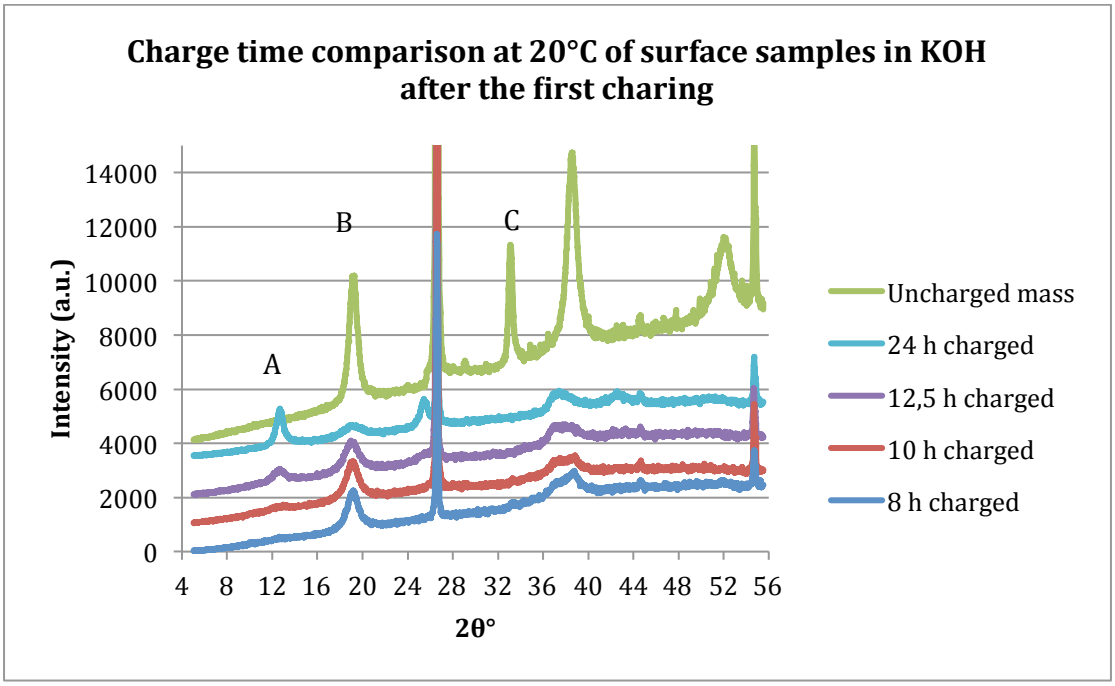

Figure 4. Diffractogram showing the nickel hydroxide phases present in the charged surface samples of different charge times at 20°C and KOH as electrolyte. The peak marked with A is the peak produced by the 001 plane of the γ-NiOOH, B is the peak produced by the 001 plane of the β-NiOOH and C is the peak produced by the 100 plane of $Ni(OH)_2$, which appears if the sample is discharged. This applies to all following diffractograms.

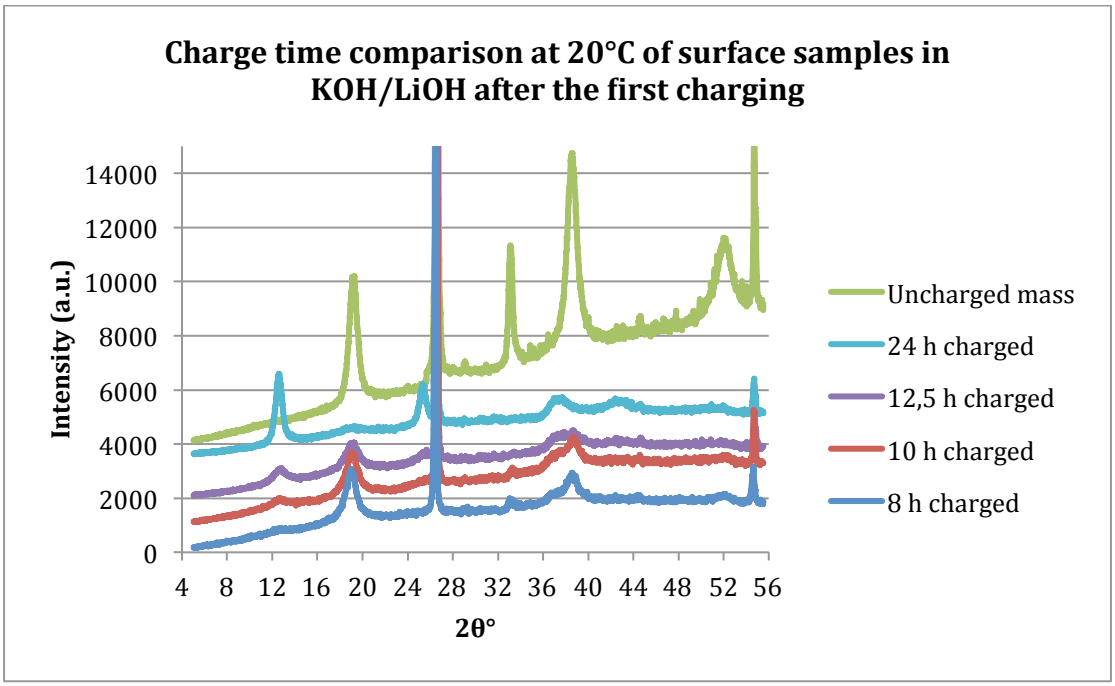

Figure 5. Diffractogram showing the nickel hydroxide phases present in the charged surface samples of different charge times at 20°C and KOH/LiOH as electrolyte.

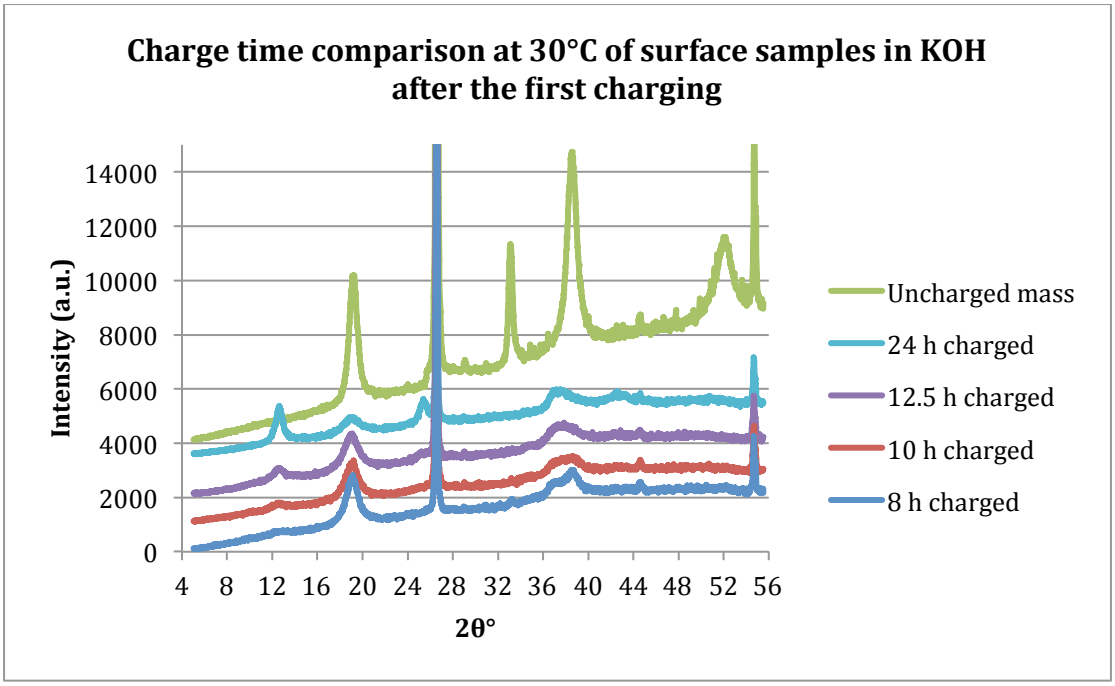

Figure 6. Diffractogram showing the nickel hydroxide phases present in the charged surface samples of different charge times at 30°C and KOH as electrolyte.

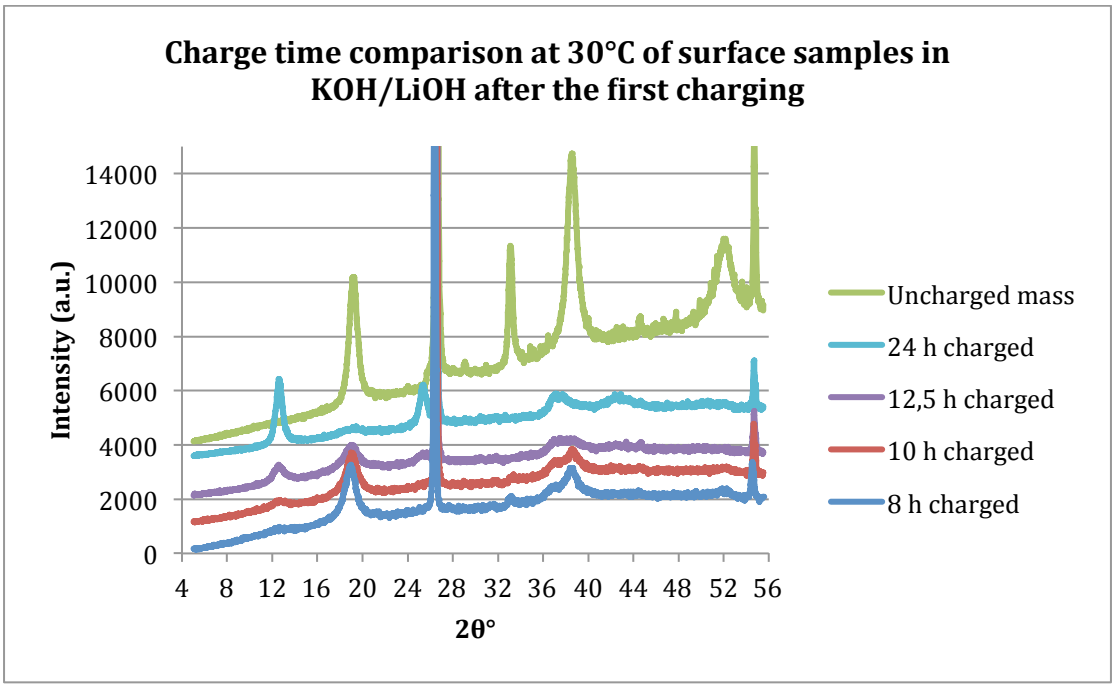

Figure 7. Diffractogram showing the nickel hydroxide phases present in the charged surface samples of different charge times at 30°C and KOH/LiOH as electrolyte.

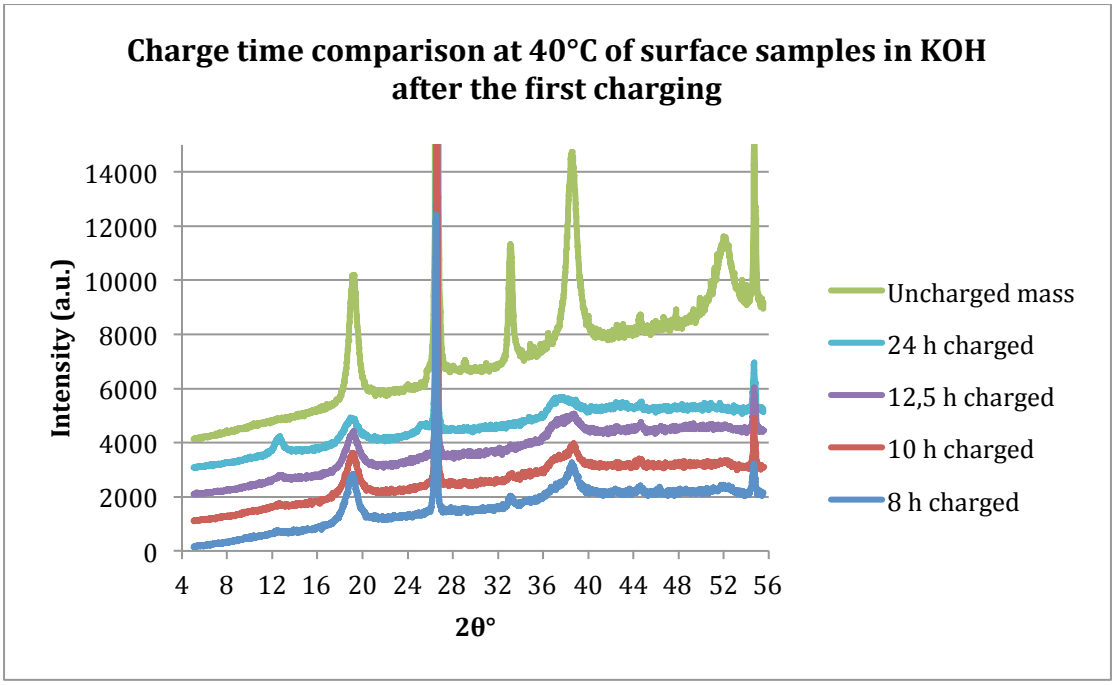

Figure 8. Diffractogram showing the nickel hydroxide phases present in the charged surface samples of different charge times at 40°C and KOH as electrolyte.

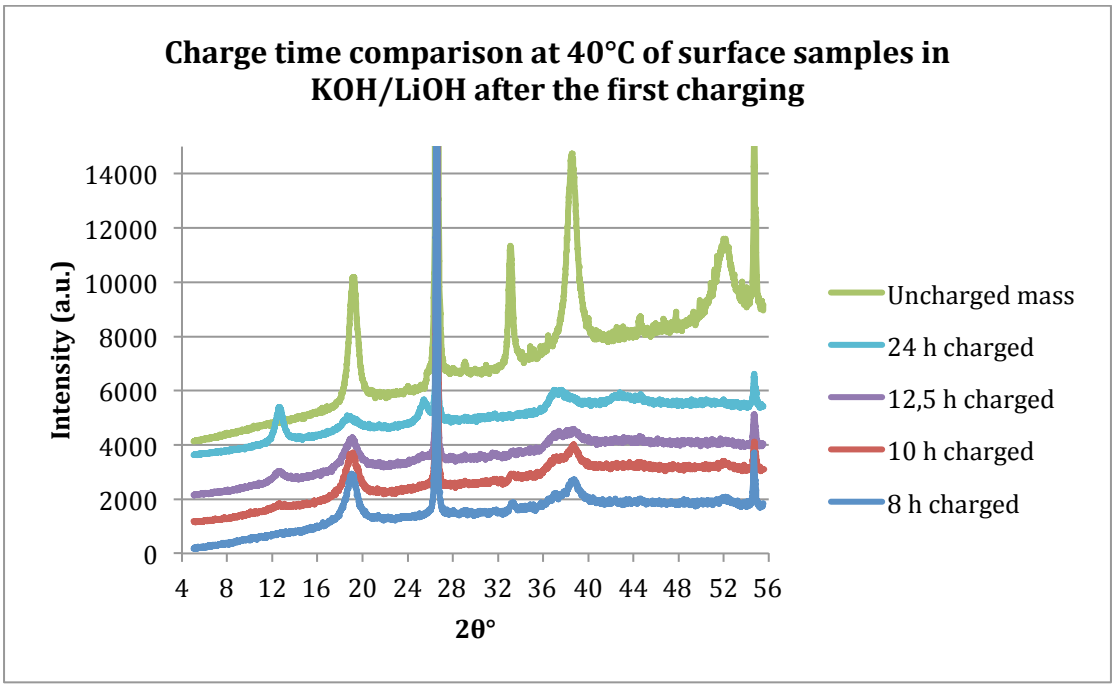

Figure 9. Diffractogram showing the nickel hydroxide phases present in the charged surface samples of different charge times at 40°C and KOH/LiOH as electrolyte.

Table 2. The area ratio between β- and γ-phase of charged samples for the different charge times, temperatures and electrolytes

		Area ratio β/γ-phase of charged samples					
		20°C		30°C		40°C	
Electrolyte	Time	Surface	Bulk	Surface	Bulk	Surface	Bulk
KOH	8 h	83	-	13	-	35	-
	10 h	6	-	9	17	15	-
	12,5 h	2	4	4	8	9	28
	24 h	0,6	0,8	0,9	2	2	5
KOH/LiOH	8 h	23	6	5	4	-	-
	10 h	5	4	10	3	12	10
	12,5 h	2	2	3	2	4	4
	24 h	0,2	0,2	0,3	0,2	1	0,7

Table 3. Remaining uncharged material appearing in form of 100 peak for the charged samples

		Uncharged material appearance of charged samples					
		20°C		30°C		40°C	
Electrolyte	Time	Surface	Bulk	Surface	Bulk	Surface	Bulk
KOH	8 h	Trace	Peak	Trace	Peak	Peak	Peak
	10 h	-	Trace	-	Trace	Trace	Peak
	12,5 h	-	-	-	-	-	Trace
	24 h	-	-	-	-	-	-
KOH/LiOH	8 h	Peak	Peak	Peak	Peak	Peak	Peak
	10 h	Trace	Peak	Trace	Peak	Trace	Peak
	12,5 h	-	-	-	-	-	-
	24 h	-	-	-	-	-	-

Third cycle discharging

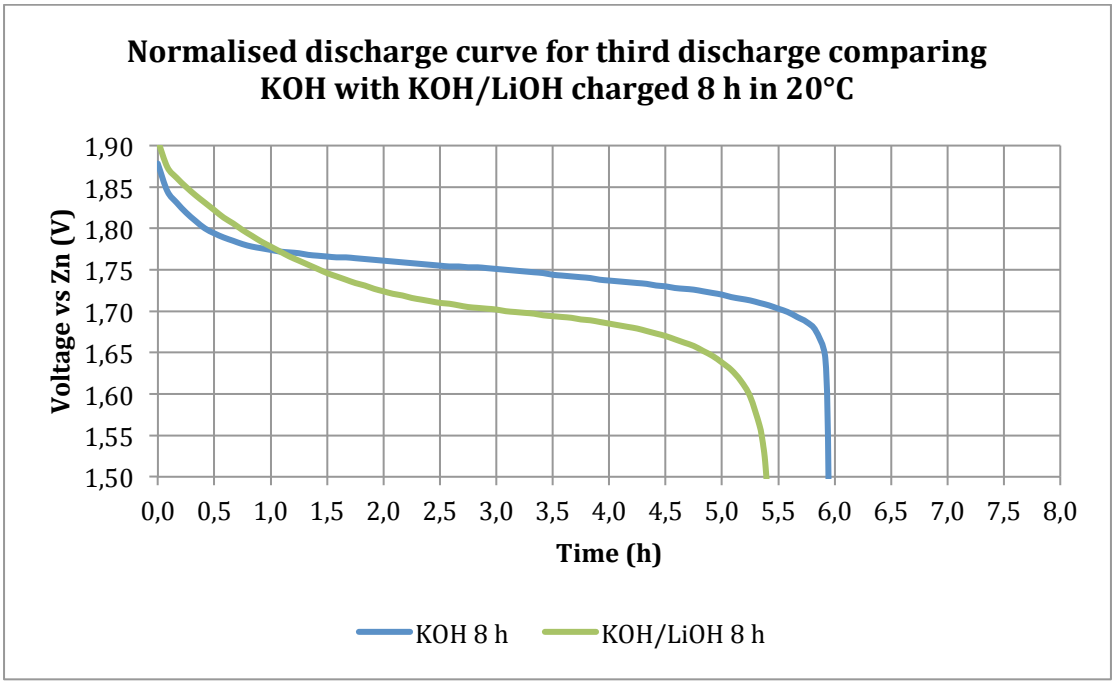

Figure 10. Normalised discharge curve for the third discharge comparing KOH with KOH/LiOH charged for 8 h in 20°C.

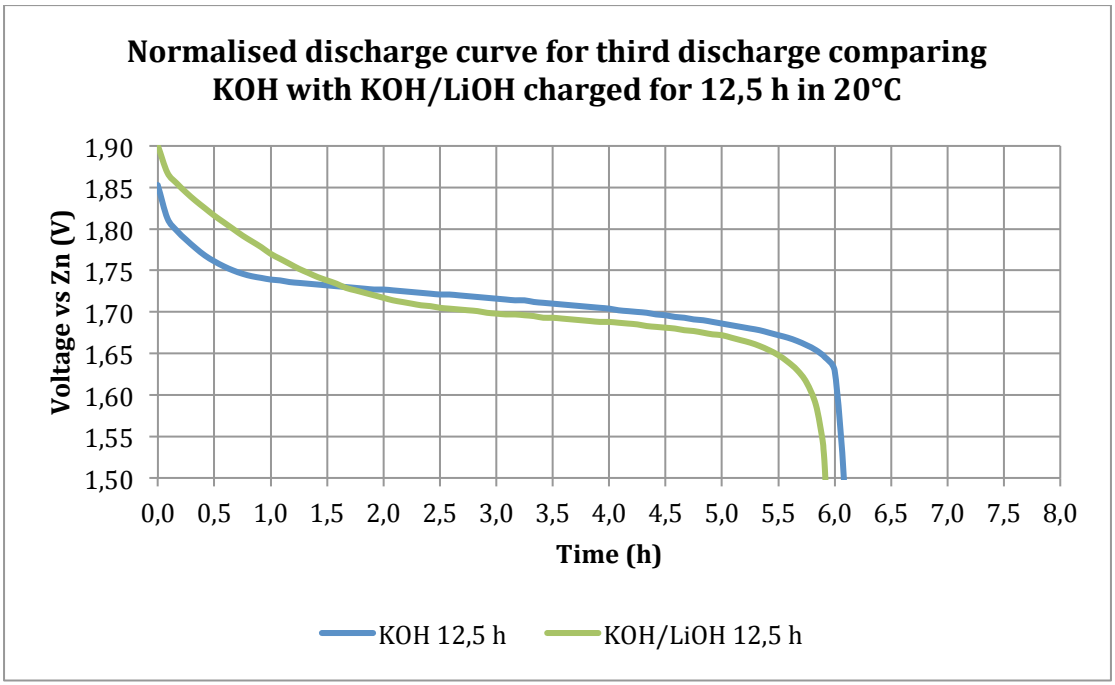

Figure 11. Normalised discharge curve for the third discharge comparing KOH with KOH/LiOH charged for 12,5 h in 20°C.

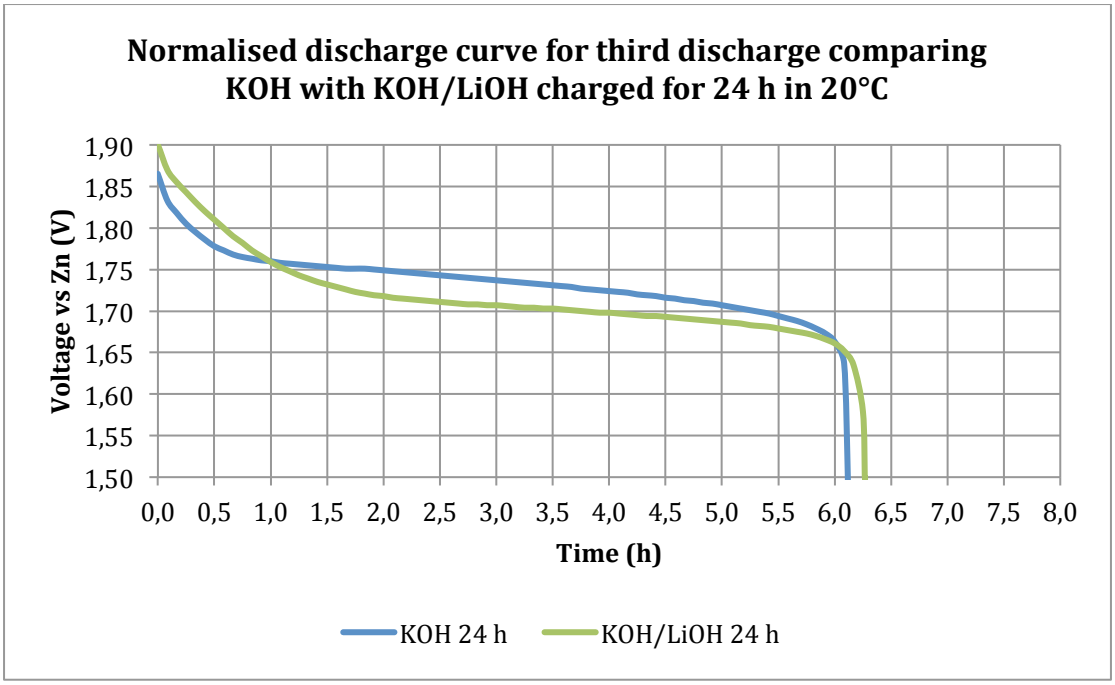

Figure 12. Normalised discharge curve for the third discharge comparing KOH with KOH/LiOH charged for 24 h in 20°C.

Table 4. Capacity of first and third cycle for the different charge times, electrolytes and temperatures

		Cycle capacity in mAh					
		20°C		30°C		40°C	
Electrolyte	Time	1st	3rd	1st	3rd	1st	3rd
KOH	8 h	512	654	504	645	448	639
	10 h	630	679	574	646	510	642
	12,5 h	642	669	658	668	613	667
	24 h	699	673	672	658	672	665
KOH/LiOH	8 h	548	593	536	585	479	561
	10 h	635	623	639	627	598	609
	12,5 h	678	651	682	646	665	637
	24 h	656	689	680	680	736	674

Table 5 Crystallite size of 001 plane after the third cycle for the different charge times, electrolytes and temperatures.

		Crystallite size of 001 direction after the third cycle in Å					
		20°C		30°C		40°C	
Electrolyte	Time	Surface	Bulk	Surface	Bulk	Surface	Bulk
KOH	8 h	86	94	79	90	84	91
	10 h	77	88	87	88	83	93
	12,5 h	77	87	73	82	80	87
	24 h	57	65	59	69	71	81
KOH/LiOH	8 h	88	88	80	76	81	81
	10 h	73	50	70	69	74	89
	12,5 h	58	54	53	55	57	64
	24 h	27	29	22	24	30	31

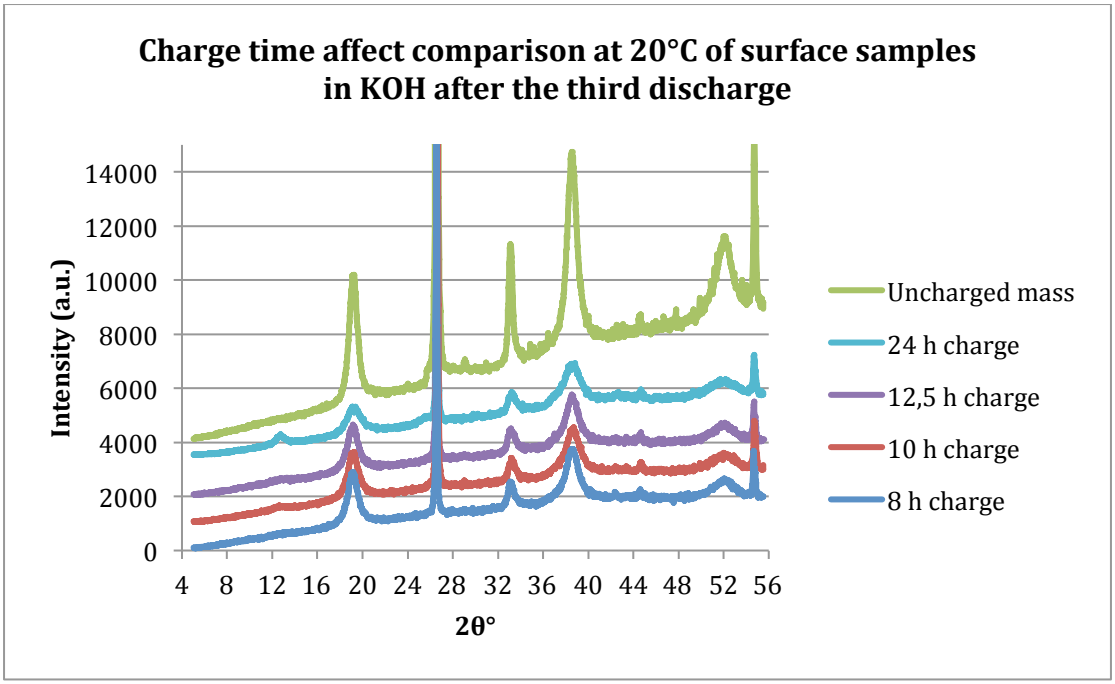

Figure 13. Diffractogram showing the nickel hydroxide phases present in the surface samples after the third discharge for the different charge times at 20°C and KOH as electrolyte.

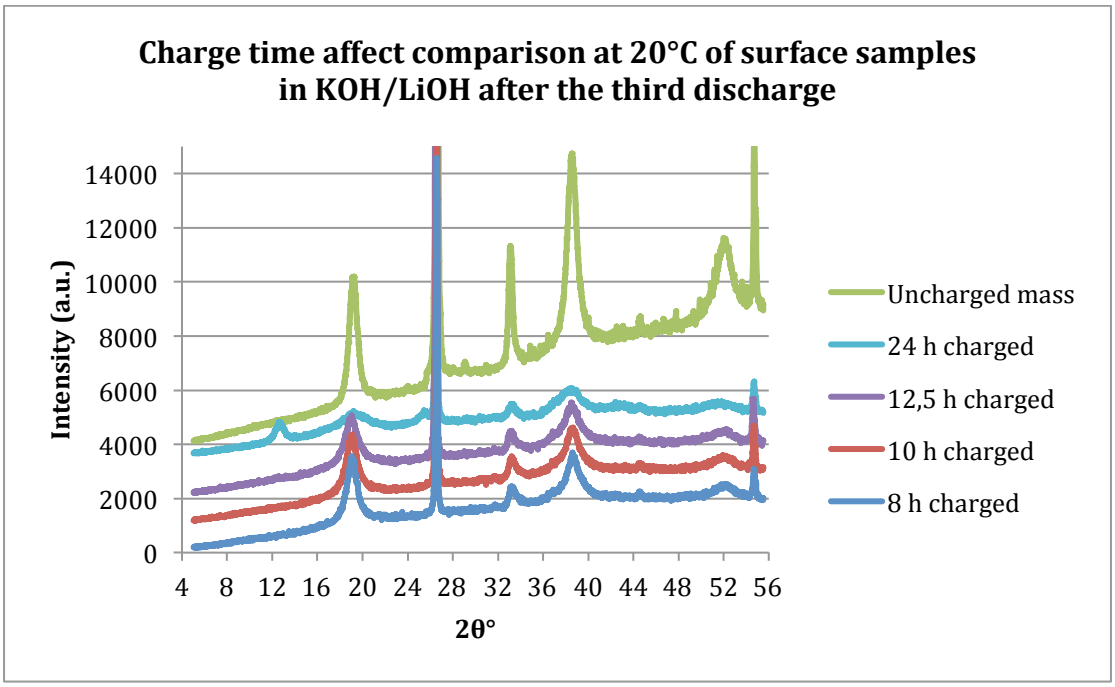

Figure 14. Diffractogram showing the nickel hydroxide phases present in the surface samples after the third discharge for the different charge times at 20°C and KOH/LiOH as electrolyte.

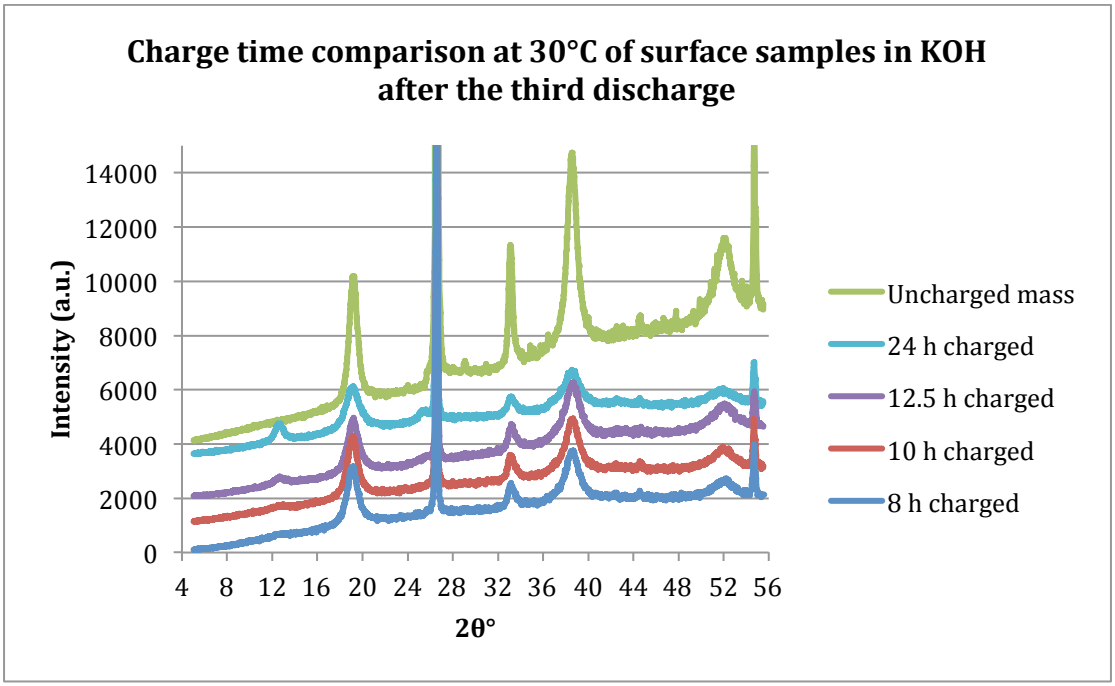

Figure 15. Diffractogram showing the nickel hydroxide phases present in the surface samples after the third discharge for the different charge times at 30°C and KOH as electrolyte.

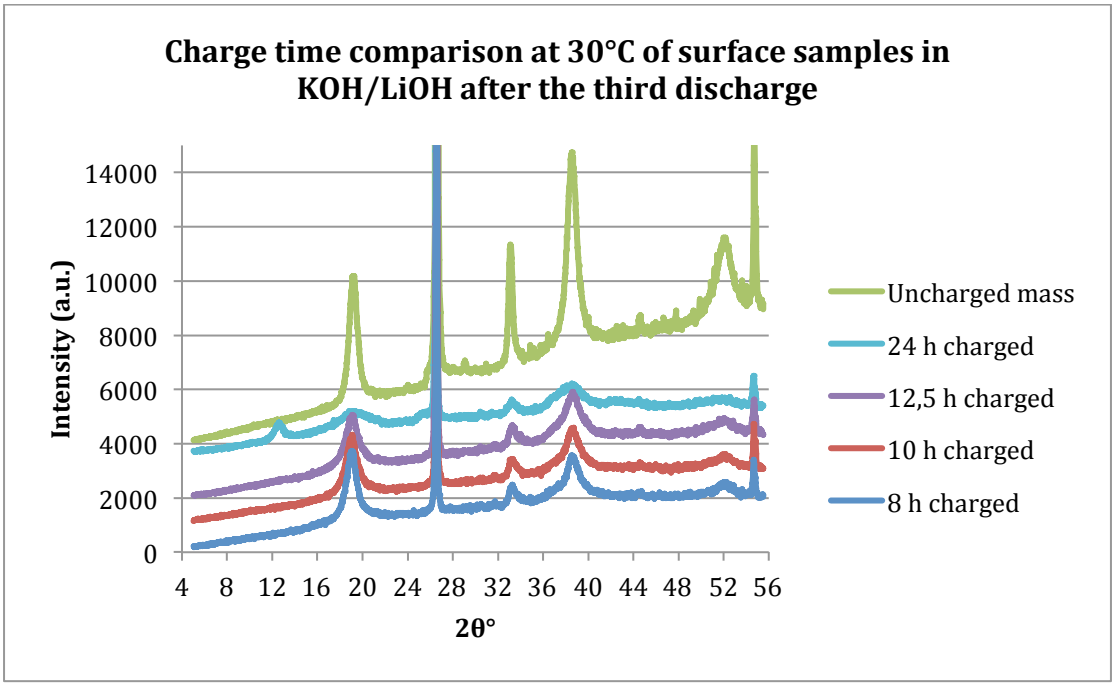

Figure 16. Diffractogram showing the nickel hydroxide phases present in the surface samples after the third discharge for the different charge times at 30°C and KOH/LiOH as electrolyte.

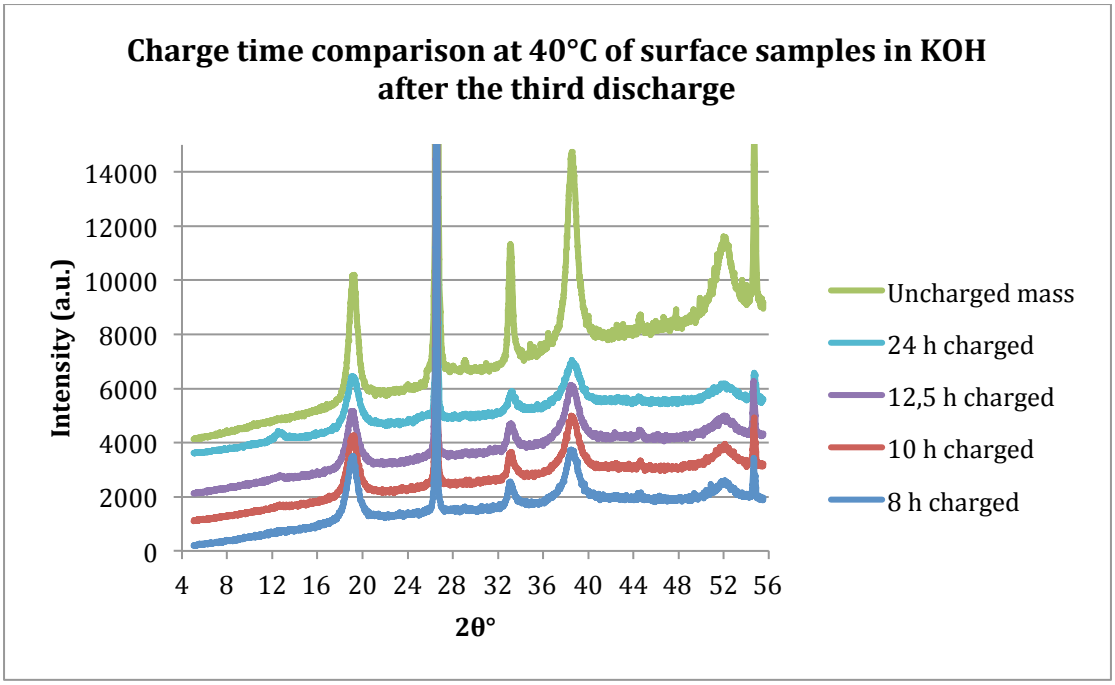

Figure 17. Diffractogram showing the nickel hydroxide phases present in the surface samples after the third discharge for the different charge times at 40°C and KOH as electrolyte.

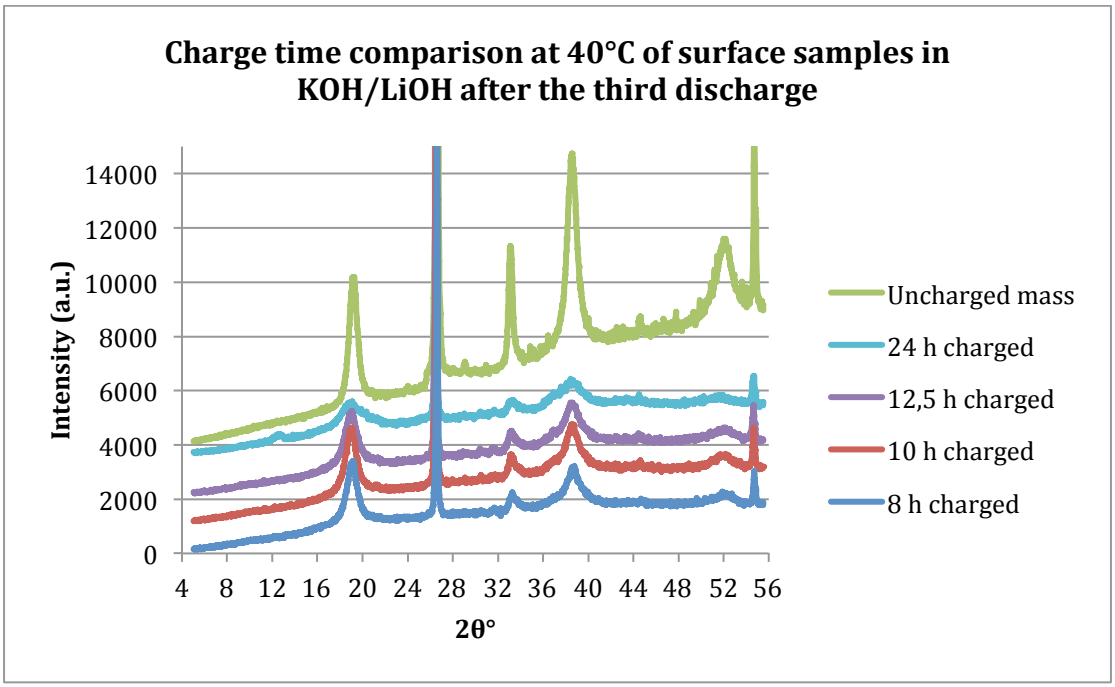

Figure 18. Diffractogram showing the nickel hydroxide phases present in the surface samples after the third discharge for the different charge times at 40°C and KOH/LiOH as electrolyte.

Table 6. Crystallite size ratio for planes 100:001 of third cycle for the different charge times, temperatures and electrolytes

		Crystallite size ratio 100:001 of the third cycle					
		20°C		30°C		40°C	
Electrolyte	Time	Surface	Bulk	Surface	Bulk	Surface	Bulk
KOH	8 h	2,5	2,1	1,6	1,7	1,8	1,9
	10 h	1,8	1,7	1,5	1,6	1,9	1,7
	12,5 h	1,7	2,2	1,9	1,6	1,7	1,8
	24 h	2,0	2,0	2,0	1,9	2,6	1,6
KOH/LiOH	8 h	1,5	1,7	1,9	1,8	1,6	2,1
	10 h	2,3	3,2	2,0	2,2	2,0	1,8
	12,5 h	2,3	2,9	2,7	2,6	2,1	2,7
	24 h	5,5	5,5	5,8	5,3	3,3	5,1

Table 7. Remaining charged material in form of γ-phase appearance in samples after the third cycle

		γ-phase appearance of the third cycle					
		20°C		30°C		40°C	
Electrolyte	Time	Surface	Bulk	Surface	Bulk	Surface	Bulk
KOH	8 h	-	-	Trace	-	-	-
	10 h	Trace	-	Trace	-	Trace	-
	12,5 h	Trace	-	Trace	Trace	Trace	-
	24 h	Peak	Peak	Peak	Peak	Peak	Trace
KOH/LiOH	8 h	-	-	-	-	-	-
	10 h	-	-	-	-	-	-
	12,5 h	-	-	-	-	-	-
	24 h	Peak	Peak	Peak	Peak	Trace	Trace

Cycling

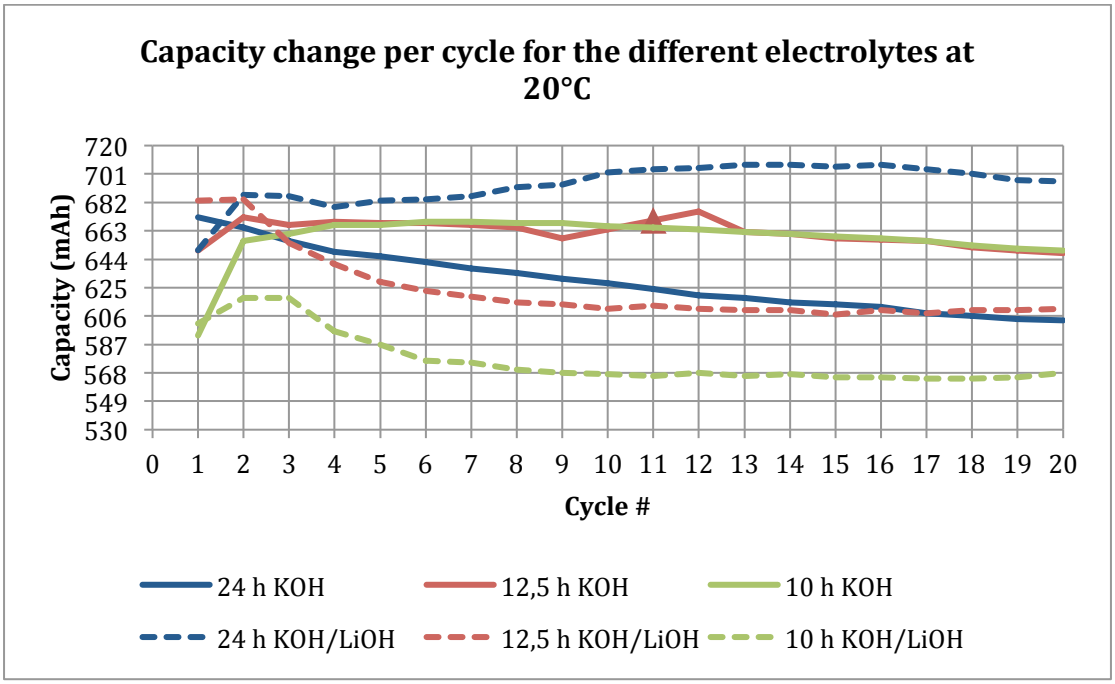

Figure 19. Graph showing the change in capacity during the different cycles at 20°C for the two electrolytes

Table 8. Crystallite size of the 001 plane after the twentieth cycle for the different charge times and electrolytes at 20°C

		Crystallite size of 001 direction after the twentieth cycle in Å	
Electrolyte	Time	Surface	Bulk
KOH	10 h	84	91
	12,5 h	78	87
	24 h	64	70
KOH/LiOH	10 h	73	73
	12,5 h	59	56
	24 h	26	30

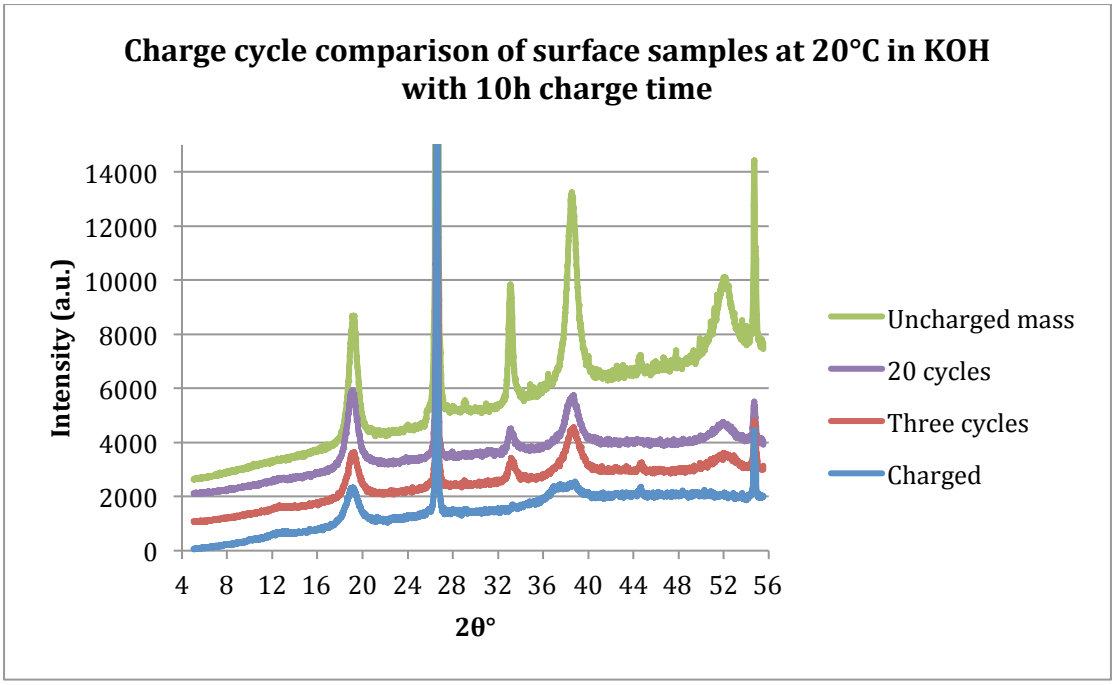

Figure 20. Diffractogram showing how the nickel hydroxide phases change during the different cycles for surface samples charged for 10 h at 20°C with KOH as electrolyte.

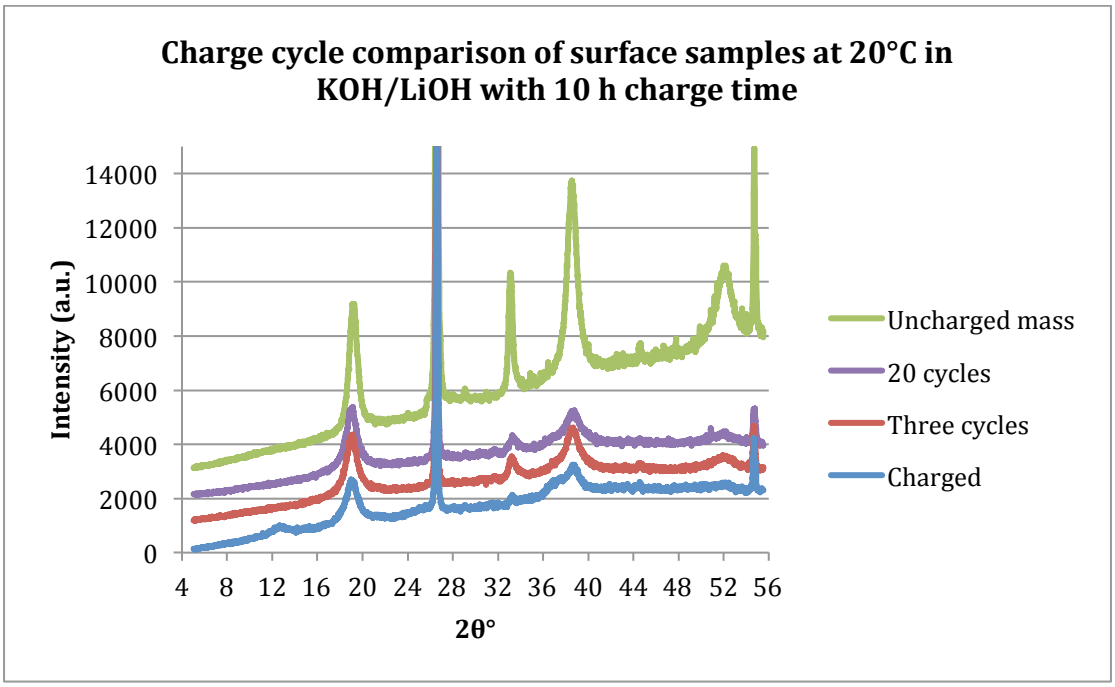

Figure 21. Diffractogram showing how the nickel hydroxide phases change during the different cycles for surface samples charged for 10 h at 20°C with KOH/LiOH as electrolyte.

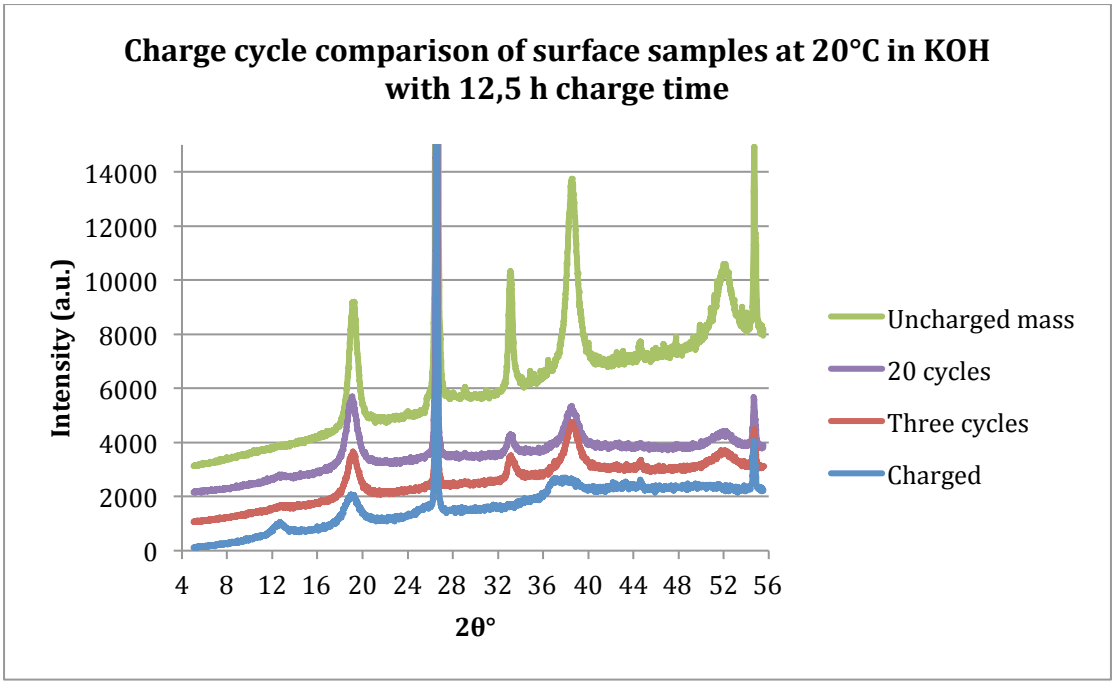

Figure 22. Diffractogram showing how the nickel hydroxide phases change during the different cycles for surface samples charged for 12,5 h at 20°C with KOH as electrolyte.

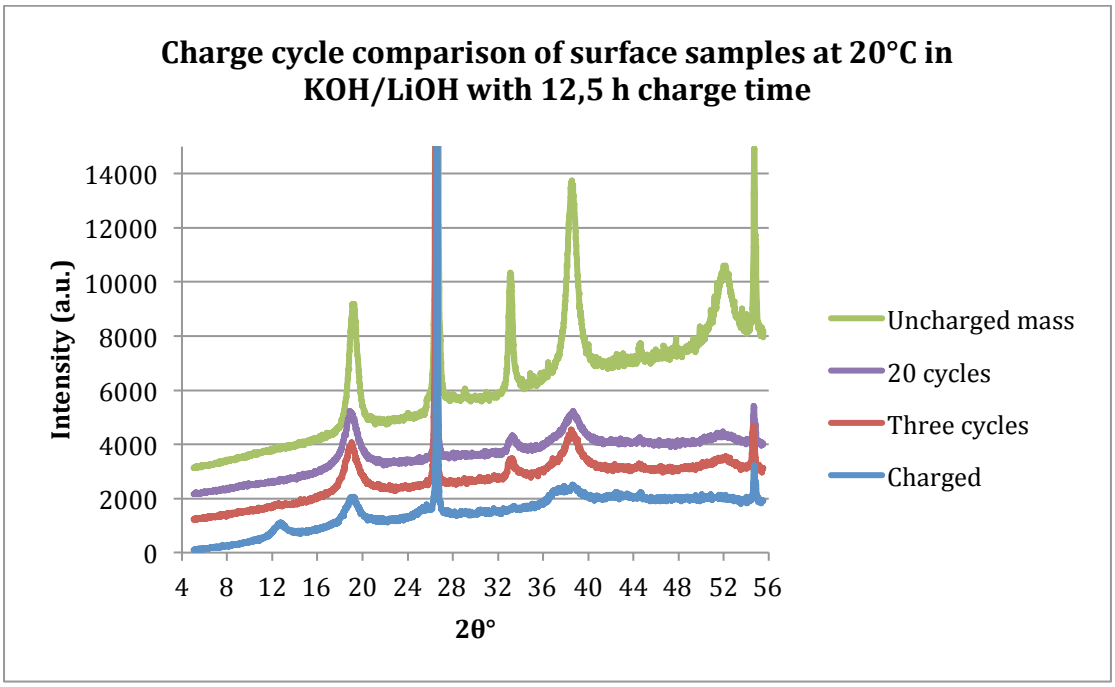

Figure 23. Diffractogram showing how the nickel hydroxide phases change during the different cycles for surface samples charged for 12,5 h at 20°C with KOH/LiOH as electrolyte.

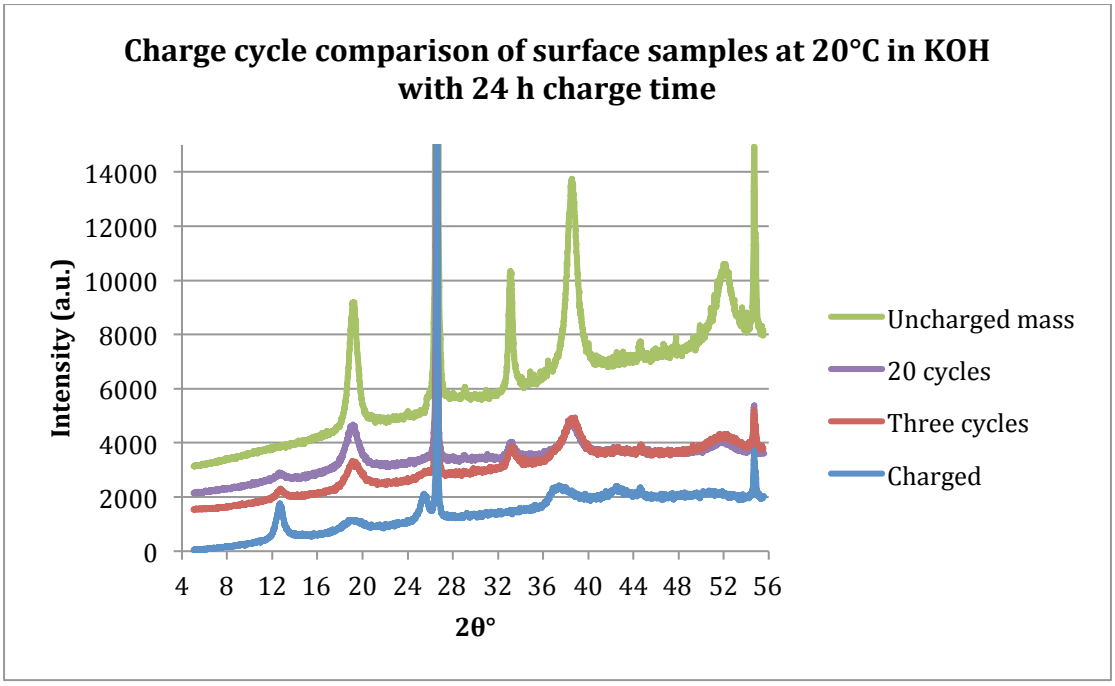

Figure 24. Diffractogram showing how the nickel hydroxide phases change during the different cycles for surface samples charged for 24 h at 20°C with KOH as electrolyte.

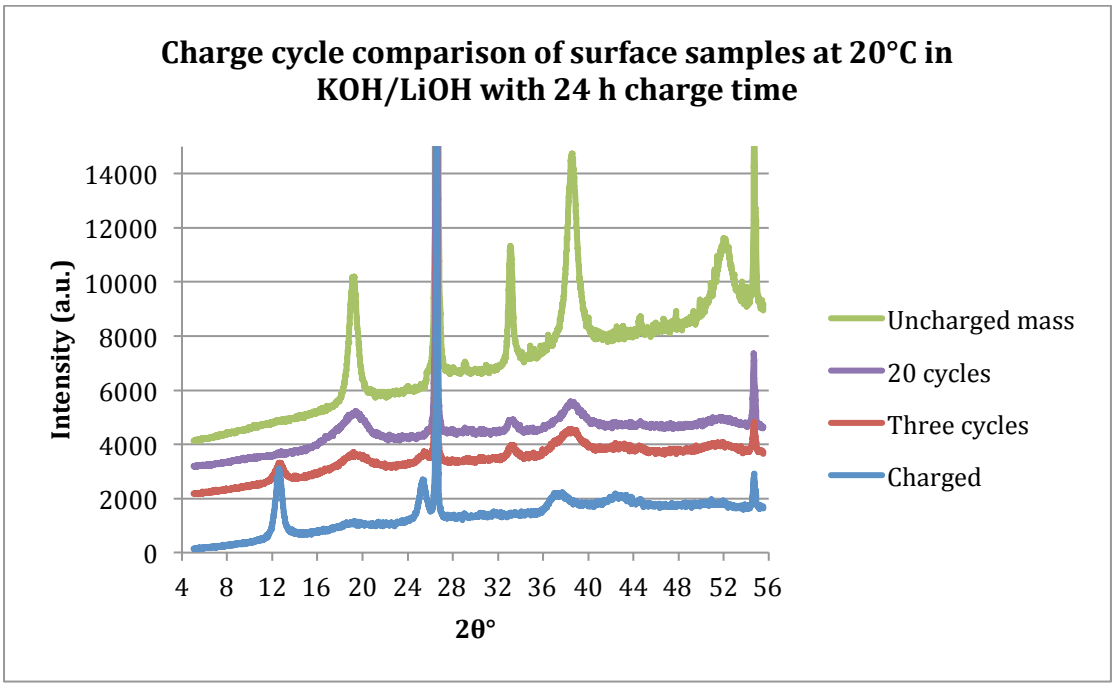

Figure 25. Diffractogram showing how the nickel hydroxide phases change during the different cycles for surface samples charged for 24 h at 20°C with KOH/LiOH as electrolyte.

Table 9. Utilization of first, third and twentieth cycle for the different charge times and electrolytes at 20°C

Electrolyte	Time	Cycle utilization in %		
		1st	3rd	20th
KOH	10 h	97,7	98,5	98,3
	12,5 h	97,9	98,4	98,3
	24 h	97,8	98,2	97,4
KOH/LiOH	10 h	97,2	98,4	97,4
	12,5 h	97,9	98,3	97,8
	24 h	97,6	98,0	97,6

Discussion

The surface samples were produced by scraping the inside of the perforated band, which made it difficult to say if the nickel mass that was collected in the mortar only came from the surface or if parts came from the bulk of the samples as well. This leads to some uncertainty of the results from these samples.
The Scherrer equation used to calculate the crystallite size could be misleading, as it does not account for disorder in the crystallite.

First cycle charging

When comparing the two electrolytes during charging at 20°C it can be seen in figure 4 and 5 that the addition of LiOH to the electrolyte increases the formation of γ-phase. This is most pronounced for the sample where the charging time was 24 h but there are some traces of γ-phase for most of the samples with LiOH in the electrolyte.

Another interesting observation is that with LiOH added to the electrolyte and charged for 24 h, the $Ni(OH)_2$ forms almost only γ-phase compared to the sample without this addition, which has some β-phase present. It can be that the β-phase of the LiOH sample is more amorphous and therefore does not show up as pronounced in the diffractogram, figure 5.

For the samples without LiOH the γ-phase seems to appear first when the charge time was 10 h or above, though for the 10 h sample it was only some small trace in the surface sample and none in the bulk. The 8 h sample with KOH as electrolyte has a β/γ ratio of 83 for the surface sample and none in bulk, which can be found in table 2, meaning there is very little γ-phase present. This might be an error as no peak or trace appears in the diffractogram, figure 4. If this is an error it has occur during the software evaluation of the diffractogram, which could be a result of the software having difficulties when evaluating so small amounts, if any.

Looking at table 3, there is a clear pattern that 8 h charge time was insufficient to fully charge the samples for both electrolytes at all examined charging temperatures, as there are noticeable amounts of uncharged material left in the samples, both in bulk and at surface.
For the samples with KOH/LiOH as electrolyte uncharged material is also present in the samples with charge time of 10 h for all temperatures. This only occurs for samples with a charging temperature of 40°C when using KOH as electrolyte, thus implying that the material has more difficulty to fully charge at that temperature. This can also be seen in table 2, where the amount of γ-phase produced in the samples with a charging time of 24 h at this temperature is lower than that generated in the samples of lower temperatures.

When looking at the temperature affect on formation of γ-phase in table 2, it can be seen that the formation decreases as the temperature increases for all samples independent of electrolyte. With an exception for the samples charged for 8 h, which behave differently for the different electrolytes. Where the samples with KOH as electrolyte has the least γ-phase at 20°C, which could be an error as mentioned before, then 40°C and last 30°C, and the samples with LiOH added to the electrolyte has the least at 40°C then 20°C and last 30°C. This is probably due to the small amounts, if any, of γ-phase present in the samples leading to difficulties for the software to evaluate the accurate area under the peaks.

Third cycle discharging

In figure 10-12, it can be seen how the LiOH affects the discharge curve of the third cycle.

The results from the capacity measurement, table 4, shows that when using KOH as electrolyte there is a falling trend in capacity with increasing temperature for samples charged for 8 and 10 hours for every cycle. Samples charged for 12,5 h have its highest capacity at 30°C and then decreases at 40°C for the first cycle, for the third cycle it experience the same falling trend as for samples with charge time 8 and 10 hours. The behaviour of the third cycle could be due to the standard charging times that were used for second and third cycle 9 and 7,5 hours respectively, which is a lot lower than the first cycles 12,5 hours. For the 24 h samples the first cycle capacity decreases when the temperature is increased to 30°C but then ramps off giving the same capacity for 40°C. The third cycle of these samples has a decreasing capacity when increasing to 30°C but then the capacity increases slightly when the temperature is increased to 40°C. Though for the samples with LiOH added to the electrolyte only the samples charged for 8 hours follows the falling trend for both first and third cycle, the other samples act a bit differently with the samples charged for 10 and 12,5 hours having the highest capacity for the first cycle at 30°C, this consists to the third cycle for the samples with 10 h charge time. For the 12,5 h samples the capacity decreases with increasing temperature for the third cycle, this also applies to the third cycle for the 24 h samples. However the samples charged for 24 hours has an increasing capacity with increasing temperature for the first cycle.

Comparing the crystallite size of the different electrolytes, see table 5, it can be seen that the samples where KOH/LiOH was used as electrolyte has a smaller crystallite size than those with KOH as electrolyte, this could be due to γ-phase inhibiting crystallite growth or the formation of $LiNiO_2$ as Li ions are present in abundance [8] and thereby inhibits crystallite growth. It is difficult to tell if either of these hypotheses is true as the peaks for $LiNiO_2$ appear in the diffractogram at the almost the same 2θ° as nickel hydroxide and nickel oxy hydroxide and for γ-phase being crystallite growth inhibiting there is just not enough data to support it.

For the crystallite size ratio after the third cycle, table 6, the electrolyte KOH shows no well-defined trend for either the affect of the charge time or the affect of the temperature for the surface samples. Though for KOH/LiOH as electrolyte the charge time affect trend is clearer with an increasing growth of 100 as the charge time increases for the surface samples. The temperature affect is however unclear with a trend that has the highest value at 30°C for all charge times except for the samples with charge time of 10 h that has a falling trend that ramps off at 30°C for the surface samples.
For the bulk samples with KOH as electrolyte the charge time affect trends are inconsequent for all temperature and the same applies for the temperature affect except for the samples with 24 h as charge time, which has a falling trend with increasing temperature. The bulk samples of KOH/LiOH have one clear charge time affect trend at 30°C, which is increasing ratio with the increasing charge time, the rest are inconsequent. For the temperature affect trends of the samples every charge time has a different trend except for the samples charged for 10 and 24 h, which both has a decreasing ratio with increasing temperature. The 8 hours samples has an increasing

ratio with increasing temperature and the 12,5 hours samples has the lowest ratio at 30°C.

When looking at the remaining γ-phase after the third cycle, table 7, it can be seen for the electrolyte KOH that γ-phase is present in the samples with charged time of 24 h and that there are some traces left in the samples charged for 10 and 12 hours for all temperature. Only 30°C show some trace of gamma-phase for the sample charged for 8 hours, which can be an error from the evaluation software as there is so small amounts, if any, of γ-phase in this sample. However for the electrolyte with LiOH addition only the samples charged for 24 hours had some γ-phase left after the third cycle for all temperatures.

Cycling

Looking at the capacity change during further cycling, figure 19, there can be seen that for the sample charged for 12,5 h in KOH the capacity increases until second cycle thereafter it stagnates or slightly decreases with each cycle. The triangle at cycle eleven of this sample marks an interpolated value of the capacity, as there was some loss of contact during this cycle.
For the sample charged for 10 h in KOH the capacity increases until the fourth cycle where it stagnates and start to resemble the curve of the 12,5 h sample.
The 24 h in KOH sample has a decreasing capacity after the first cycle, which leads to a much lower end capacity than both the 10 and 12,5 h samples. This could be due to the swelling of the γ-phase leading to a loss of contact with the active material, resulting in a lower capacity [3].
The KOH/LiOH samples behave a little differently, the 12,5 h sample starts out slightly stagnant with cycle one and two almost yielding the same capacity then decreasing for every cycle thereafter.
For the sample with charge time of 10 h, the capacity increases to the second cycle and then stagnates to the third cycle followed by a decreasing capacity with increasing number of cycles.
The 24 h charged sample on the other hand has an increasing capacity from cycle one to two and then the capacity slightly increases with increasing number of cycles.

When looking at the diffractograms of what phases are present during the different cycles for the different electrolytes, figure 20-25, it can be seen that for all KOH/LiOH samples the gamma-phase decreases with increasing number of cycles. This could be the reason for the 24 h sample to have an increasing capacity, as the γ-phase would exchange 1,6 electrons instead of 1 electron for the β-phase. If this would be the case it is a bit strange that the samples with 10 and 12,5 hours did not experience the same behaviour, though this might be explained by these samples having less γ-phase to begin with and thereby depleting it earlier than the 24 h sample.
For the KOH samples it can be noticed that for both samples charged for 10 and 12,5 h the γ-phase seems to be gone by the twentieth cycle, but for the 24 h sample it still remains trace of γ-phase after the twentieth cycle. This might be due to the swelling connected to the γ-phase, leading to loss in contact with active material and the remaining γ-phase being unable to reduce back to β-phase nickel hydroxide.

The crystallite size during the cycling tests, table 8, shows a decreasing crystallite size with increasing charge time for both electrolytes. Though it also shows the same trend

as for the discharging tests, where the electrolyte with LiOH additions give rise to smaller crystallite sizes than the electrolyte without it.

Conclusion

The aim of this thesis work was to establish the different trends that show up when subjecting the nickel hydroxide to the different conditions. Therefore it seemed to be sufficient to test singles of every sample.

It can be found that the electrolyte with LiOH addition produces more γ-phase and smaller crystallite sizes for all samples compared to the samples exposed to the electrolyte without this addition.

For the temperature test it is difficult to deduce a clear pattern for all samples, but it seems for 40°C to be some difficulties of charging for the pure KOH electrolyte, providing lower amounts of γ-phase in the 24 h sample and traces of uncharged material even for the 12,5 h sample. The LiOH containing electrolyte handled the temperatures better with higher capacities than the pure KOH electrolyte for the first cycle and higher temperatures, which was predictable, as literature has stated that it would improve temperature performance of the electrode [3]. Though the crystallite size of the samples charged for 24 h in KOH/LiOH has the largest size at 40°C and the highest capacity, which contradicts previous studies [10].

The charge times affect for both electrolytes shows an increasing capacity with increasing time, but also increasing amount of γ-phase and a lowering of crystallite size. For the 24 h samples with KOH as electrolyte it could also be seen that they had lower capacity after the third discharge than the 12,5 h samples, this is probably due to the swelling associated with the γ-phase.

The cycling tests showed that samples cycled in KOH as electrolyte had remains of γ-phase left even after twenty cycles, but the samples cycled in KOH/LiOH had no γ-phase left after the twentieth cycle, and some samples had converted the γ-phase as early as in the third cycle. It also showed that the capacity of the samples with KOH as electrolyte either increased in the beginning and then plateaued or decreased with each cycle. For the samples with LiOH added to the electrolyte showed a different trend for the capacity behaviour per cycle. Both samples charge for 10 h and 12,5 h showed an increase for the first two cycles then decreased for the following cycles. The sample charged for 24 h showed an increasing capacity with increasing number of cycles. In figure 25, it can be seen that this sample has remains of γ-phase left after the third cycle. With further cycling the amount of γ-phase decreases suggesting that the increasing capacity could be from a conversion of the γ-phase as it exchange 1,6 electrons instead of 1 electron for the β-phase. For the 24 h KOH sample the capacity decreased for each cycle suggesting that the active material has lost contact due to the swelling associated with the γ-phase.

There were no major difficulties with the methods used in this work, just some inexperience of work with the software used to evaluate the diffractograms in the beginning. This changed with the multiple evaluations done during this work, but some diffractograms could have been re-evaluated for more exact results.

The surface samples were produced by scraping the inside of the perforated band, which made it difficult to be certain that it was only the active material closest to the electrolyte that was examined and not parts originating from the bulk.

Future work

For future work it could be interesting to look a bit further into what happens with the samples that used KOH/LiOH as electrolyte, did $LiNiO_2$ form, how could it produce so much γ-phase and use it so efficiently and why does it produce smaller crystallite sizes.

References

1. Song, Q.S., Li, Y.Y. and Chan S.L.I. 2005. Physical and electrochemical characteristics of nanostructured nickel hydroxide. *Journal of Applied Electrochemistry,* vol. 35, issue 2. pp. 157-162.
2. Chen, J., Bradhurst, D.H., Dou, S.X. and Liu, H.K. 1999. Nickel hydroxide as an active material for the positive electrode in rechargeable alkaline batteries. *Journal of The Electrochemical Society,* vol. 146, issue 10. pp. 3606-3612.
3. Bernard, Patrick. 2009. Nickel-Cadmium: Sealed. In: Juergen Garche, Chris Dyer, Patrick Moseley, Zempachi Ogumi, David Rand and Bruno Scrosati, editor. *Encyclopedia of Electrochemical Power Sources,* vol. 4. Amsterdam: Elsevier. pp. 459-481.
4. Sjövall, Rune. 2015. SAFT AB. Personal communications.
5. Sundvall, Christian. 2013. *Development of Methods for Creation and Characterization of an Oxidation Stable Cobalt Hydroxide.* Masters thesis, Lund University.
6. Smart, Lesley E. and Moore, Elaine A. 2012. *Solid State Chemistry: An Introduction.* Fourth edition. Boca Raton: CRC Press Taylor & Francis Group.
7. Kalyani, P. and Kalaiselvi, N. 2005. Various aspects of $LiNiO_2$ chemistry: A review. *Science and Technology of Advanced Materials,* 6:6. pp. 689-703.
8. Thirsk, H. R. 1974. *Specialist Periodical Reports: Electrochemistry,* vol. 4. London: The Chemistry Society Burlington House. pp. 41-42.
9. Falk, Uno S. and Salkind, Alvin J. 1969. *Alkaline Storage Batteries.* New York: John Wiley & Sons.
10. Bernard, M.C., Cortes, R., Keddam, M., Takenouti, H., Bernard, P. and Senyarich, S. 1996. Structural defects and electrochemical reactivity of β-$Ni(OH)_2$. *Journal of Power Sources,* vol. 63. pp. 247-254.

Appendix A

Calculation of maximum theoretical capacity of nickel hydroxide for one electron. Equation used,

$$q = \frac{n \cdot F}{3600 \cdot M}\ mAh/g$$

q = capacity
n = moles of electrons
F = Faraday's constant
M = molar mass of nickel hydroxide

For the calculation,

n = 1
M = 92, 724 g/mol
F = 96485,33 C/mol
C = A*s

$$q = \frac{1 \cdot 96485{,}33}{3600 \cdot 92{,}724} \approx 289{,}04 \cdot 10^{-3} Ah/g$$

q = 289,04 mAh/g

Appendix B

Discharge

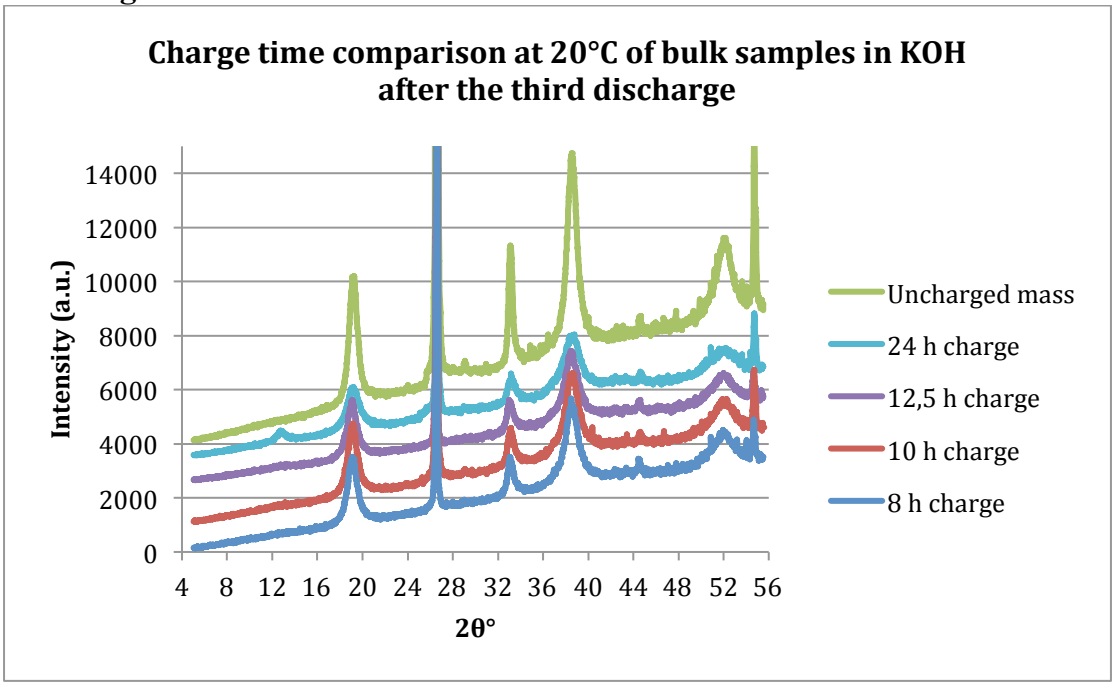

Figure 26. Diffractogram showing the nickel hydroxide phases present in the bulk samples after the third discharge for the different charge times at 20°C and KOH as electrolyte.

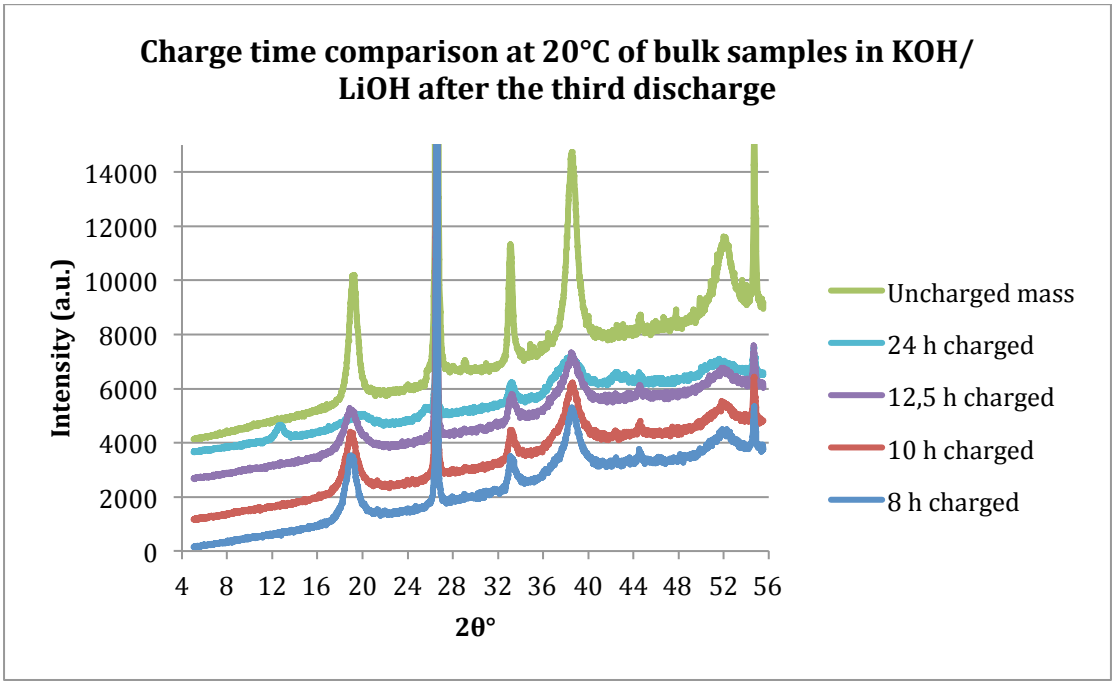

Figure 27. Diffractogram showing the nickel hydroxide phases present in the bulk samples after the third discharge for the different charge times at 20°C and KOH/LiOH as electrolyte.

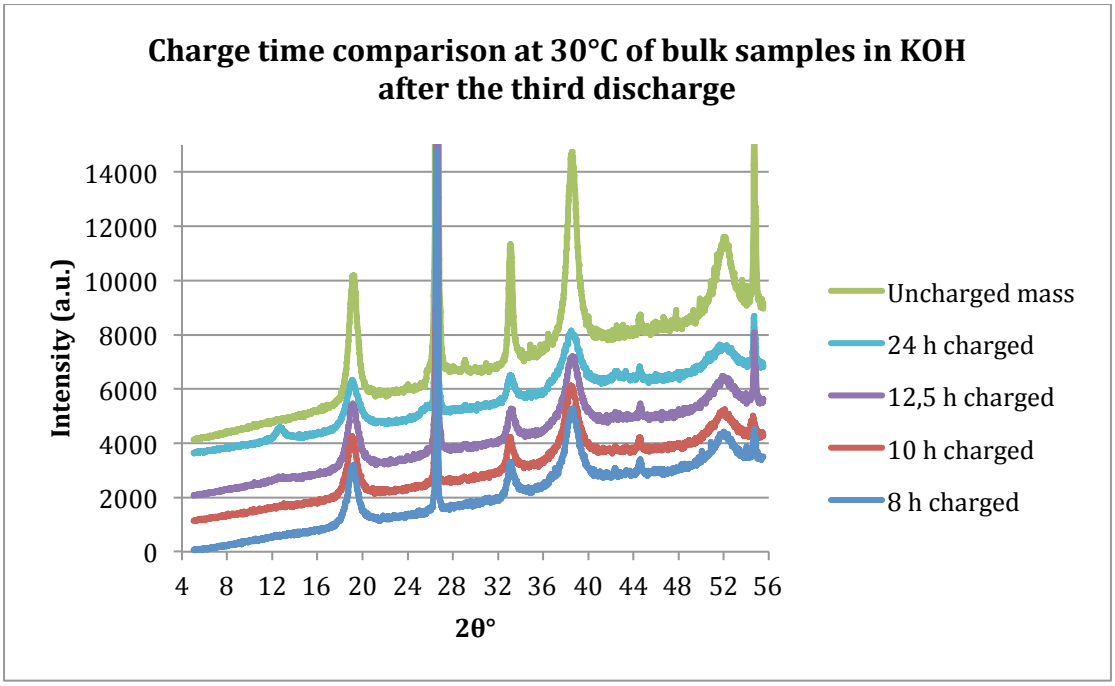

Figure 28. Diffractogram showing the nickel hydroxide phases present in the bulk samples after the third discharge for the different charge times at 30°C and KOH as electrolyte.

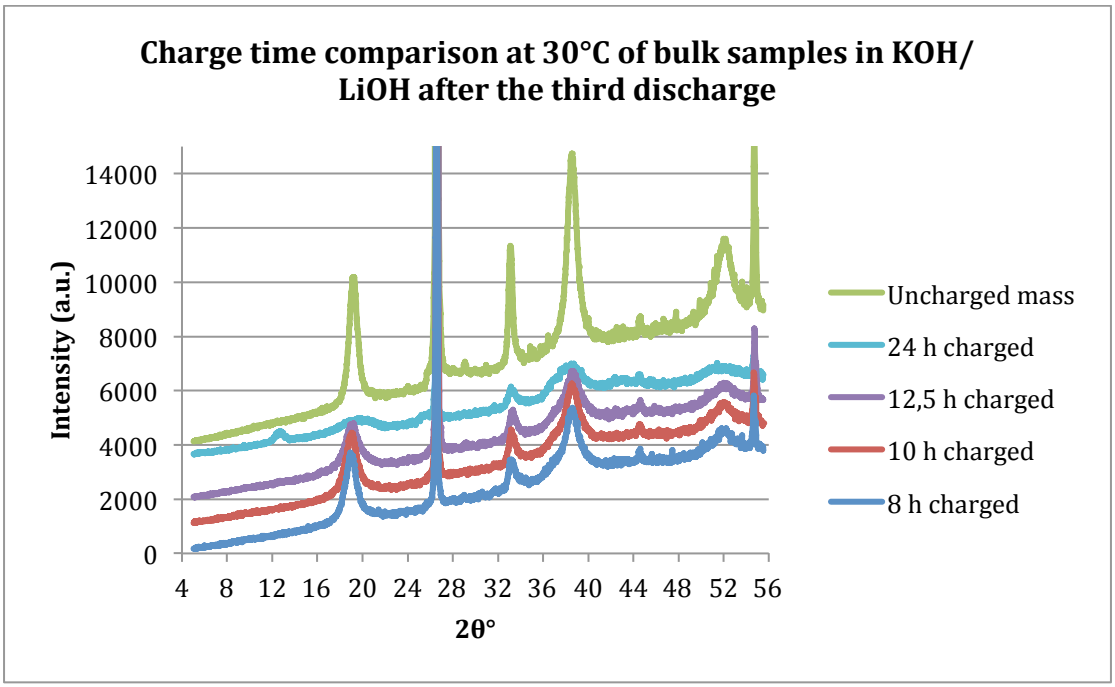

Figure 29. Diffractogram showing the nickel hydroxide phases present in the bulk samples after the third discharge for the different charge times at 30°C and KOH/LiOH as electrolyte.

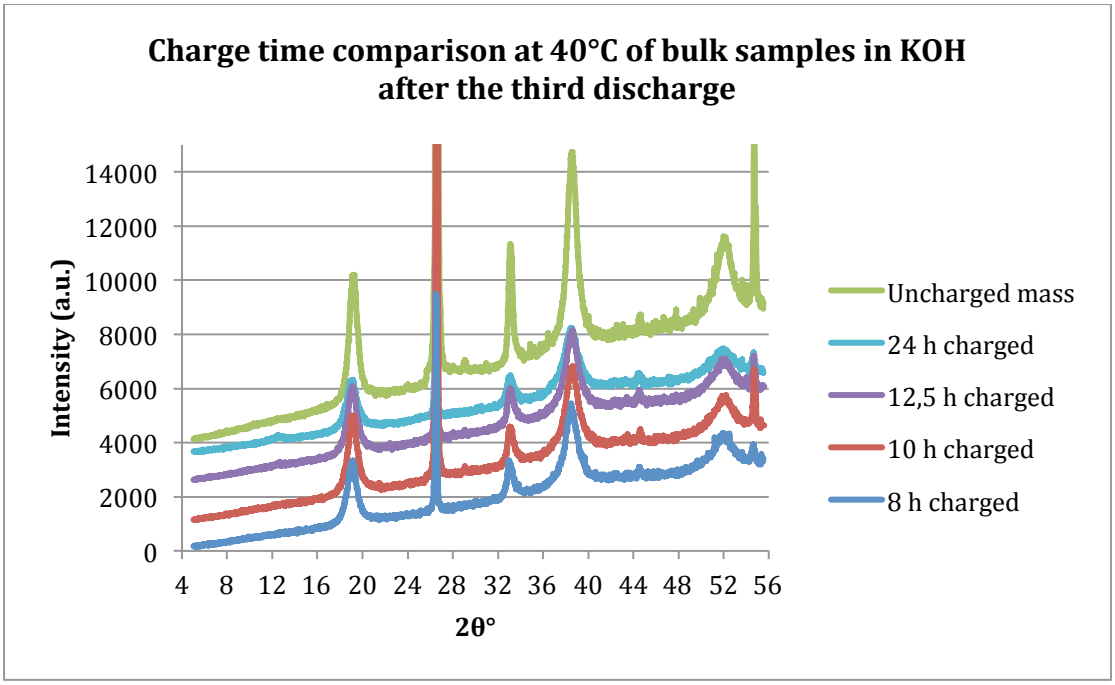

Figure 30. Diffractogram showing the nickel hydroxide phases present in the bulk samples after the third discharge for the different charge times at 40°C and KOH as electrolyte.

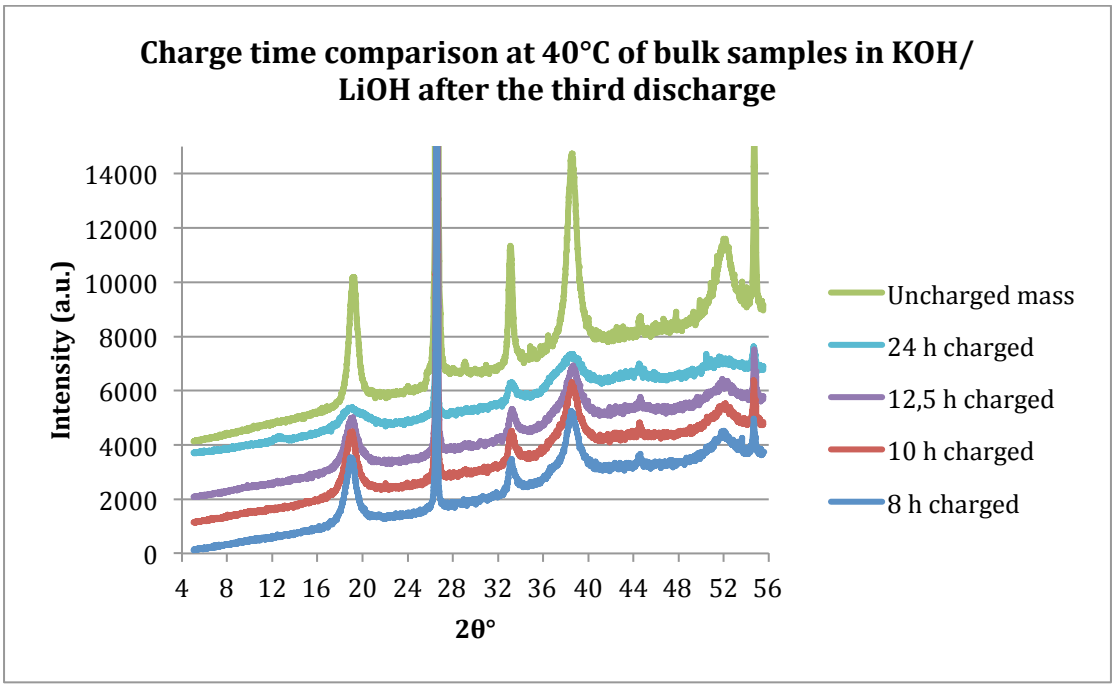

Figure 31. Diffractogram showing the nickel hydroxide phases present in the bulk samples after the third discharge for the different charge times at 40°C and KOH/LiOH as electrolyte.